PCP
PLANT & CELL PHYSIOLOGY

Identification of miRNAs and Their Targets in the Liverwort *Marchantia polymorpha* by Integrating RNA-Seq and Degradome Analyses

Pin-Chun Lin[1,13], Chia-Wei Lu[1,13], Bing-Nan Shen[1], Guan-Zong Lee[1], John L. Bowman[4], Mario A. Arteaga-Vazquez[5], Li-Yu Daisy Liu[6], Syuan-Fei Hong[1], Chu-Fang Lo[7], Gong-Min Su[1], Takayuki Kohchi[8], Kimitsune Ishizaki[9], Sabine Zachgo[10], Felix Althoff[10], Mizuki Takenaka[11], Katsuyuki T. Yamato[12] and Shih-Shun Lin[1,2,3,*]

[1]Institute of Biotechnology, National Taiwan University, Taipei, Taiwan 106
[2]Agricultural Biotechnology Research Center, Academia Sinica, Taipei, Taiwan 115
[3]Center of Biotechnology, National Taiwan University, Taipei, Taiwan 106
[4]School of Biological Sciences, Monash University, Melbourne, Australia
[5]Instituto de Biotecnologia y Ecologia Aplicada (INBIOTECA), Universidad Veracruzana, Xalapa Veracruz, Mexico
[6]Department of Agronomy, National Taiwan University, 1 Sec. 4, Roosevelt Rd. Taipei, Taiwan 106
[7]Institute of Bioinformatics and Biosignal Transduction, National Cheng Kung University, Taiwan 701
[8]Graduate School of Biostudies, Kyoto University, Kyoto, 606-8502 Japan
[9]Graduate School of Science, Kobe University, Kobe 657-8501 Japan
[10]University of Osnabrück, Botany Department, D-49076 Osnabrück, Germany
[11]Universität Ulm, Molekulare Botanik, D-89069 Ulm, Germany.
[12]Faculty of Biology-Oriented Science and Technology, Kinki University, Nishimitani, Kinokawa, Wakayama, 649-6493 Japan.
[13]These authors contributed equally to this work.
*Corresponding author: E-mail, linss01@ntu.edu.tw; Fax, +886-2-33666001.
(Received September 5, 2015; Accepted November 22, 2015)

Bryophytes (liverworts, hornworts and mosses) comprise the three earliest diverging lineages of land plants (embryophytes). *Marchantia polymorpha*, a complex thalloid Marchantiopsida liverwort that has been developed into a model genetic system, occupies a key phylogenetic position. Therefore, *M. polymorpha* is useful in studies aiming to elucidate the evolution of gene regulation mechanisms in plants. In this study, we used computational, transcriptomic, small RNA and degradome analyses to characterize microRNA (miRNA)-mediated pathways of gene regulation in *M. polymorpha*. The data have been integrated into the open access ContigViews-miRNA platform for further reference. In addition to core components of the miRNA pathway, 129 unique miRNA sequences, 11 of which could be classified into seven miRNA families that are conserved in embryophytes (miR166a, miR390, miR529c, miR171-3p, miR408a, miR160 and miR319a), were identified. A combination of computational and degradome analyses allowed us to identify and experimentally validate 249 targets. In some cases, the target genes are orthologous to those of other embryophytes, but in other cases, the conserved miRNAs target either paralogs or members of different gene families. In addition, the newly discovered Mpo-miR11707.1 and Mpo-miR11707.2 are generated from a common precursor and target Mp*ARGONAUTE1* (LW1759). Two other newly discovered miRNAs, Mpo-miR11687.1 and Mpo-miR11681.1, target the MADS-box transcription factors Mp*MADS1* and Mp*MADS2*, respectively. Interestingly, one of the *pentatricopeptide repeat* (*PPR*) gene family members, Mp*PPR_66* (LW9825), the protein products of which are generally involved in various steps of RNA metabolism, has a long stem–loop transcript that can generate Mpo-miR11692.1 to autoregulate Mp*PPR_66* (LW9825) mRNA. This study provides a foundation for further investigations of the RNA-mediated silencing mechanism in *M. polymorpha* as well as of the evolution of this gene silencing pathway in embryophytes.

Keywords: ARGONAUTE • Class III homeodomain leucine zipper • Degradome • MADS-box • *Marchantia polymorpha* • miRNA prediction • Transcriptome.

Abbreviations: AGO1, ARGONAUTE 1; ARF2, AUXIN RESPONSE FACTOR 2; AtACD2, ACCELERATED CELL DEATH2; AtEDM2, ENHANCED DOWNY MILDEW2; AtPHT2,1, PHOSPHATE TRANSPORTER 2,1; AtRD21, RESPONSIVE TO DEHYDRATION21; AtSPL, SQUAMOSA PROMOTER BINDING PROTEIN-LIKE; AtSTOP1, SENSITIVE TO PROTON RHIZOTOXICITY1; AtVIP4, VERNALIZATION INDEPENDENCE4; CDS, coding sequence; DCL1, DICER-LIKE 1; EMBL, European Molecular Biology Laboratory; GO, Gene Ontology; HEN1, HUA ENHANCER1; HYL1, HYPONASTIC LEAVES 1; JGI, Joint Genome Institute; lncRNA, long non-coding RNA; LRR, leucine-rich repeat; miRNA, microRNA; MpC3HDZ1, CLASS III HOMEODOMAIN LEUCINE ZIPPER1; MpEF1α. elongation factor promoter 1α: NGS, next-generation sequencing; ORF, open reading frame; phasiRNA, phased secondary small RNA; PPR. pentatricopeptide repeat; pre-miRNA, precursor miRNA; pri-miRNA, primary

Plant Cell Physiol. 57(2): 339–358 (2016) doi:10.1093/pcp/pcw020, Advance Access publication on 9 February 2016, available online at www.pcp.oxfordjournals.org

transcript; RdDM, RNA-directed DNA methylation; RISC, RNA-induced silencing complex; RT–PCR, reverse transcription–PCR; SE, SERRATE, siRNA, short interfering RNA; Tak1, Takaragaike-1; tasiRNA, *trans*-acting small interfering RNA; TF, transcription factor; TGH, TOUGH; UTR, untranslated region; YFP, yellow fluorecent protein.

The raw transcriptome reads, small RNAs and degradome reported in this paper have been submitted to the NCBI Short Read Archive under accession numbers SRR2179938 (transcriptome of *M. polymorpha*), SRR2179617 (small RNAs of *M. polymorpha*) and SRR2179371 (degradome of *M. polymorpha*). The transcriptome contig sequences and miRNA information are available in the ContigViews database (contigviews.bioagri.ntu.edu.tw).

Introduction

Embryophytes colonized land approximately 480 million years ago (Kenrick and Crane 1997, Qiu et al. 2006, Gensel 2008, Ligrone et al. 2012). Bryophytes (liverworts, hornworts and mosses) comprise the earliest diverging land plant lineages. While the phylogenetic relationships among bryophytes remain enigmatic, the fossil record and evidence from systematics, molecular and phylogenetic studies suggest that the first plants that colonized terrestrial environments possessed attributes of liverworts (Mishler and Churchill 1984, Kenrick and Crane 1997, Bowman 2013). Studies of microRNAs (miRNAs) in plant species, such as *Marchantia polymorpha* at key evolutionary nodes hold great promise for increasing our understanding of the evolution of miRNA biogenesis and function. Although only a few miRNAs are conserved across land plant lineages, including the moss *Physcomitrella patens*, the lycopod *Selaginella moellendorffii* and angiosperms (e.g. *Arabidopsis thaliana* and *Oryza sativa*), it has been shown that diverse, lineage-specific small RNAs may perform common biological functions (Axtell et al. 2007, Cuperus et al. 2011).

MiRNAs are endogenous, small, non-coding RNAs of 20–24 nucleotides (nt) in length that regulate gene expression via a post-transcriptional silencing mechanism that depends on the complementarity between the miRNA and a target mRNA (Lee et al. 1993, Wightman et al. 1993, Reinhart et al. 2002, Chen 2009, Rogers and Chen 2013). In angiosperms, the majority of genes encoding miRNAs are transcribed by RNA polymerase II (Aukerman and Sakai 2003, Kim et al. 2011) and processed from double-stranded RNA (dsRNA) precursors. The activity of DICER-LIKE 1 (DCL1) in combination with TOUGH (TGH; a G-patch domain protein), HYPONASTIC LEAVES 1 (HYL1; a dsRNA-binding protein) and SERRATE (SE; a zinc finger protein) is required for processing the miRNA primary transcript (pri-miRNA) and precursor miRNA (pre-miRNA), and release of the miRNA/miRNA* duplex (miRNA* is the complementary strand of the miRNA in the duplex) (Rogers and Chen 2013). HUA ENHANCER1 (HEN1; a 2′-*O*-methyltransferase) is required for methylation at the 3′ end of the miRNA/miRNA* duplex (Yang et al. 2006). Loading of the miRNA into the RNA-induced silencing complex (RISC), where ARGONAUTE 1 (AGO1) plays a fundamental role as an effector (Baumberger and Baulcombe 2005, Mallory and Vaucheret 2010), provides the sequence specificity needed to locate the target mRNA. Depending on the degree of complementarity between the miRNA and the target mRNA, the RISC can induce either target silencing or translation inhibition (Chen 2009, Rogers and Chen 2013). MiRNAs play essential roles in numerous developmental processes and responses to environmental challenges (Chen 2009, Chen 2012). In addition to miRNAs, short interfering RNAs (siRNAs) and phased secondary small RNAs (phasiRNAs), originally designated as *trans*-acting small interfering RNAs (tasiRNAs), also have significant roles in plants. SiRNAs that are 23–25 nt in length target homologous genomic DNA sequences for cytosine methylation and histone modifications through a phenomenon known as RNA-directed DNA methylation (RdDM) (Law and Jacobsen 2010, Matzke and Mosher 2014). RdDM is involved in silencing invasive nucleic acids, including repetitive genomic regions and transposable elements (Matzke et al. 2015). PhasiRNAs (including tasiRNAs) are a class of siRNAs that are produced in a phased pattern from non-coding transcripts (*TAS* transcripts) by miRNA activity (Peragine et al. 2004, Vazquez et al. 2004, Allen et al. 2005, Yoshikawa et al. 2005, Fei et al. 2013). The biogenesis of phasiRNAs involves the activity of proteins distinct from those involved in miRNA and siRNA biogenesis (Fei et al. 2013, Yoshikawa 2013). TasiRNAs are conserved from mosses to flowering plants; one example is the regulatory circuit involving miR390 and *TAS3a* that regulates auxin responses and phase change by targeting *AUXIN RESPONSE FACTOR 2* (*ARF2*), *ARF3* and *ARF4* (Allen et al. 2005, Williams et al. 2005, Fahlgren et al. 2006, Hunter et al. 2006, Marin et al. 2010, Fei et al. 2013).

In a transcriptome study of *M. polymorpha*, 33,692 expressed sequence tags were generated from immature male and female sexual organs to identify sex-determining genes (Nagai et al. 1999, Nishiyama et al. 2000). Sharma et al. (2014) studied whole-transcriptome profiles from vegetative thalli as well as from immature and mature sexual organs and generated 46,533 contigs by de novo assembly (the N_{50} lengths were 757 and 471 bp, respectively, based on various assemblers). In a miRNA study of *P. patens* and *S. moellendorffii*, 280 and 64 mature miRNAs were identified, respectively, and registered in miRBase (version 21) (Kozomara and Griffiths-Jones 2011, Zimmer et al. 2013). Moreover, miRNAs and their targets in *Pellia endiviifolia*, a Jungermanniopsida liverwort, have been reported (Alaba et al. 2015). These miRNAs were identified through small RNA cloning (Axtell et al. 2007, Fattash et al. 2007, Krasnikova et al. 2013) and next-generation sequencing (NGS) approaches (Kozomara and Griffiths-Jones 2011, Zimmer et al. 2013). These bryophyte transcriptome and miRNA profiles provide useful information for studies of miRNA evolution in embryophytes.

Bona fide miRNAs can be discovered through the detection of both the miRNA and the cleaved complementary miRNA targets using RNA degradome sequencing (Addo-Quaye et al. 2008, German et al. 2008, Gregory et al. 2008). The degradome

has been analyzed via a high-throughput approach involving the sequencing of the 5′ ends of uncapped RNA fragments on a genome-wide scale. This approach has been widely used for miRNA/target predictions (Cao et al. 2014, Yang et al. 2015, Yao et al. 2015) and validation in diverse plant species, including those without a reference genome (Addo-Quaye et al. 2008, German et al. 2009, Bracken et al. 2011, Jeong et al. 2013, Yang et al. 2013). We found evidence for pri-miRNAs giving rise to more than one pre-miRNA and also for a precursor that can produce multiple miRNAs. All together, in this study we identified a set of 129 unique miRNAs (118 unique sequence novel miRNAs and 11 sequences that can be grouped into seven conserved miRNA families) generated from 71 different pre-miRNAs that are processed from 62 pri-miRNAs. We obtained statistically significant evidence of miRNA-mediated cleavage for 171 target genes and 78 undefined transcripts using our miRNA/target prediction pipeline. In addition, we show that integrating the degradome profile into the pipeline improved the accuracy of our miRNA/target prediction. Embryophyte evolution and several important miRNAs and target genes of *M. polymorpha* are highlighted and discussed in this article.

Results

Whole-transcriptome analysis and gene annotation in *M. polymorpha*

Poly(A) RNA purified from total RNA of 4-week-old *M. polymorpha* thalli (accession Takaragaike-1; Tak1) was used for library generation and transcriptome analysis by deep sequencing (**Fig. 1A**). Eighty-four million reads were obtained from transcriptome sequencing, and 39,090 contig sequences were de novo assembled using the CLC Genome Workbench (version 5.1). The N_{50} of these contigs was 1,962 nt (**Table 1**). The ContigViews-transcriptome system (www.contigviews.bioagri.ntu.edu.tw/publish/list?type=transcriptome) can automatically determine the integrity of a gene in terms of the presence of a complete open reading frame (ORF) (Liu et al. 2014). After ORF annotation, we identified 4,890 potentially full-length mRNAs (12.5% of the contigs) with both 5′- and 3′-untranslated regions (UTRs) and a complete ORF (**Table 1**; **Fig. 1B**).

The average size of *M. polymorpha* ORFs is similar to that observed in Arabidopsis (**Fig. 1C**). However, the average amino acid sequence similarity between *M. polymorpha* and Arabidopsis is <20% (**Fig. 1D**). In addition, 11.7% of the contigs (4,573 transcripts) represent partial mRNAs, which lack the 5′ end and/or the 3′ end and encode a partial ORF (**Table 1**; **Fig. 1B**). Interestingly, 75.8% of the contigs (29,627 transcripts) showed no identifiable ORF similarity when compared with the Arabidopsis or European Molecular Biology Laboratory (EMBL) coding sequence (CDS) databases. Some of these transcripts might belong to novel genes not yet reported. However, some of these transcripts might be portions of long UTRs or encode either long non-coding RNAs (lncRNAs) or rRNAs. Therefore, we defined such transcripts as undefined transcripts (**Table 1**; **Fig. 1B**). In summary, the sequence of 39,090 contigs can be used to search for potential miRNA precursors, while 9,463 annotated genes can be used to identify miRNA targets. As a reference, contig identifications (IDs) of *M. polymorpha* transcripts in the ContigViews database were labeled with the prefix 'LW' (indicating liverwort) followed by a serial number; for example, the ID of the Mp*AGO1* gene is LW1759. In addition, official gene IDs of *M. polymorpha*, which were announced by the Joint Genome Institute (JGI) and which correspond to these contigs, are listed in **Supplementary Tables S1** and **S2**.

MiRNA prediction in *M. polymorpha*

To achieve sampling consistency, all libraries (mRNA, small RNA and degradome) originated from the same batch of total RNA. Regarding the size distribution of small RNAs, most small RNAs ($>2.6 \times 10^6$) were 21 nt in length the second largest group ($\sim 1.3 \times 10^6$) contains small RNAs of 22 nt in length and approximately 1×10^6 small RNAs were 24 nt in length (**Fig. 1E**). **Fig. 2A** shows the workflow for miRNA and target prediction. All predictions were performed using RNAfold, psRNATarget and ContigViews web servers (Dai and Zhao 2011, Liu et al. 2014).

The RNA secondary structures of all 39,090 contig sequences were generated with the RNAfold algorithm accessed via the Vienna RNA web server (rna.tbi.univie.ac.at). Small RNAs mapped against contig sequences showing perfect identity to the stem region of predicted stem–loop structures were selected and potential miRNAs and miRNA*s were filtered based on established criteria for annotation of plant miRNAs including the presence of a 3′-end overhang of 0–3 nt (**Fig. 2B**) (Bartel 2004, Lai et al. 2004, Kim and Nam 2006). We employed a combination of in silico prediction with psRNATarget (**Fig. 2A**) and experimental validation by degradome analysis. ContigViews was used to analyze the degradome profile further, and targets were selected based on the presence of a statistically significant degradome peak (t-plot) at the 10th and 11th positions on the target site. All the miRNA and target information, including transcript expression and degradome profiles, was integrated as a database in the open access ContigViews-miRNA system (www.contigviews.bioagri.ntu.edu.tw/publish/list?type=miRNA).

We evaluated whether integrating the degradome profile can enhance the accuracy of miRNA and target prediction. In total, 10,966 species (reads >1) of 12.6×10^6 small RNA species were shown to be located on the hairpin stem. The 10,966 small RNA species were used as miRNA candidates to predict their targets using psRNATarget without integrating the degradome profile, resulting in 8,403 of the 10,966 small RNA species having potential targets. However, after integrating the degradome profile, only 1,287 of the 8,403 species of small RNAs showed a significant degradome signal at the target site; thus, the degradome profile improves the accuracy of the miRNA and target prediction and might remove false-positive results.

Following the analysis, 1,287 species of small RNAs were merged into 129 miRNA species derived from 71 pre-miRNAs that were generated from 62 pri-miRNAs (**Supplementary Table S1**). Fifty-three of 129 unique miRNA sequences could

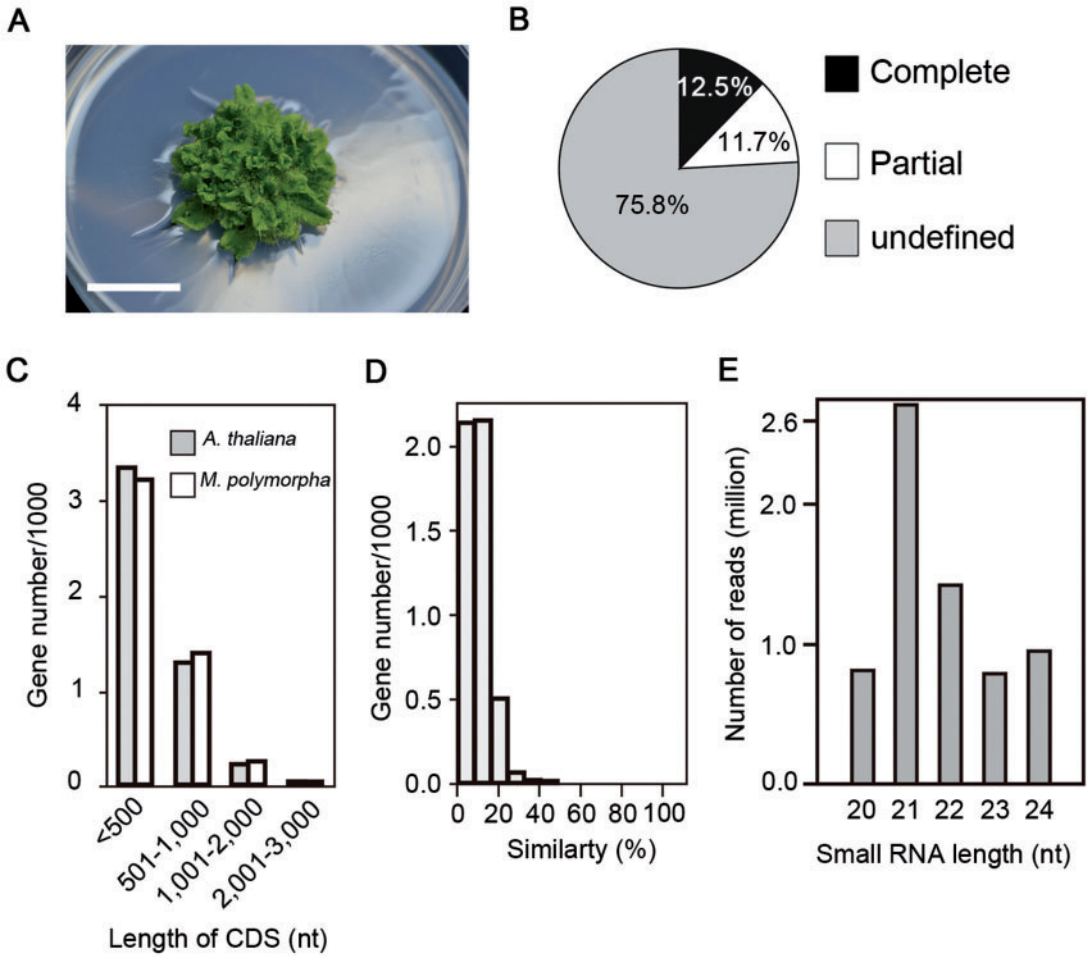

Fig. 1 Characterization of the *Marchantia polymorpha* transcriptome and the annotation of open reading frames (ORFs). (A) Four-week-old *M. polymorpha* plants (Tak1 accessions). Scale bar = 2 cm. (B) Pie chart showing the percentages of full-length transcripts (12.5%), partial transcripts (11.7%) and undefined transcripts (75.8%) from the 39,090 de novo assembled *M. polymorpha* contigs. (C) Gene length distribution comparison between *M. polymorpha* and *Arabidopsis thaliana*. Only the coding DNA sequences (CDS) of full-length transcripts were calculated. (D) Amino acid similarity of the CDS from Arabidopsis and *M. polymorpha*. (E) Size distribution of small RNAs in *M. polymorpha*.

Table 1 Summary of the sequenced transcriptome assembly and gene annotation results

***Marchantia polymorpha* transcriptome**	
Raw reads	84,890,386 reads
De novo assembled contigs[a]	39,090 contigs
N_{50} of de novo assembled contigs	1,962 nt
Complete gene	4,890 genes (12.5%)
Partial gene	4,573 genes (11.7%)
Undefined transcript	29,627 contigs (75.8%)

[a] CLC Genome Workbench 5.1 was used for de novo assembly of the *M. polymorpha* transcriptome.

be classified into 23 miRNA families (**Supplementary Table S3**). Moreover, these Mp*MIR* genes have been mapped to the *M. polymorpha* genome, and all precursors (62 precursors) were found in the genome. Raw reads of the *M. plymorpha* genome (SRR1899537) that were generated by the JGI were downloaded from the Sequence Read Archive (SRA) of the National Center for Biotechnology Information (NCBI), and drafts of genome contigs were de novo assembled by ABySS (version 1.3.4; k-mer 64) and CLC (version 7.1; k-mer 64) and used for Mp*MIR* gene mapping. These findings confirmed the accuracy of miRNA prediction.

In general, we found that some pre-miRNAs can generate > 1 miRNA. For instance, pre-Mpo-miR529c generates three miRNA species, Mpo-miR529c.1, Mpo-miR529c.2 and Mpo-miR529c.3, which have respective targets (**Supplementary Fig. S29**; **Supplementary Table S1**). We evaluated the first 5′-end nucleotide of *M. polymorpha* miRNAs and found that 'U' most often serves as the first 5′-end nucleotide (46.5%), whereas 'A', 'C' and 'G' are the first 5′-end nucleotide in 18.6%, 20.2% and 14.7% of cases, respectively (**Fig. 2C**).

Target prediction in *M. polymorpha*

Marchantia polymorpha miRNAs can target and cleave 171 mRNAs and 78 undefined transcripts with a significant degradome peak ($P < 0.01$) at a given predicted target cleavage position (between the 10th and 11th positions in the target site)

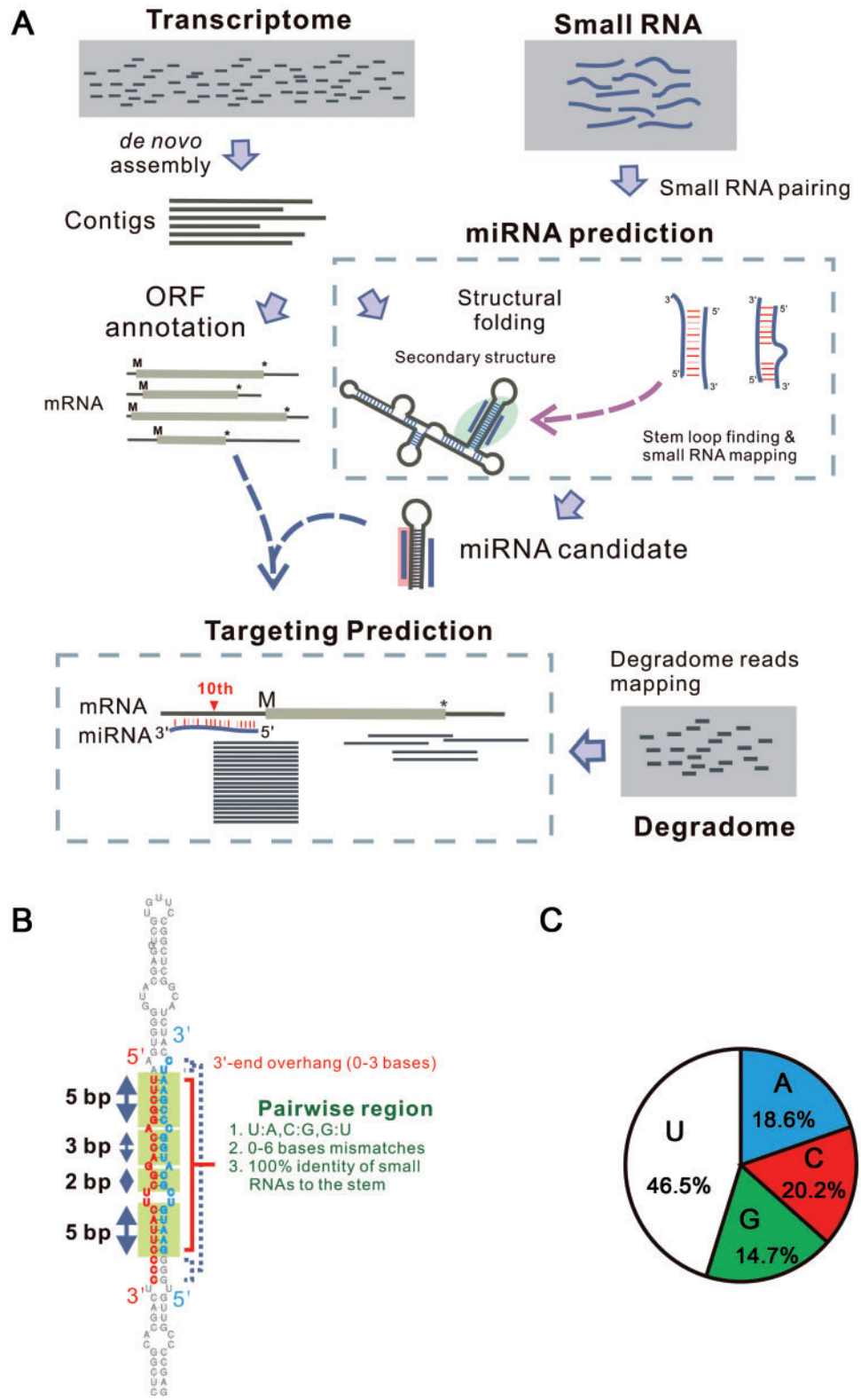

Fig. 2 RNA-Seq workflow for miRNA–target prediction in *Marchantia polymorpha*. (A) Four-week-old thalli of *M. polymorpha* were selected for whole-transcriptome, small RNA and degradome analyses using deep sequencing. The ContigViews platform was employed to annotate open reading frames (ORFs) from a set of 39,090 de novo assembled *M. polymorpha* contigs. RNA secondary structure was predicted with the RNAfold program from the Vienna RNA web server. MiRNA target prediction was performed with the psRNATarget web server. (B) The algorithm for miRNA prediction. (C) Pie chart illustrating the distribution of the first 5′-end nucleotides of *M. polymorpha* miRNA.

(**Supplementary Table S1**; **Supplementary Figs. S1–S88**). Notably, with the exception of five contigs that were not in the JGI gene model, the other 166 contigs were assigned JGI gene IDs (**Supplementary Table S1**). In addition, **Supplementary Table S2** lists names of homologs of *M. polymorpha* target genes from Arabidopsis or other species and their functions. We analyzed these targets by gene family annotation using ContigViews and found that 26.4% of the targets (24 of 91 annotated functional genes) were transcription factor (TF) genes (**Supplementary Fig. S89A**). The second largest group comprised miscellaneous membrane-associated genes. These results suggest that TF genes are the major miRNA targets in *M. polymorpha* (**Supplementary Fig. S89A, B**). We also analyzed the Gene Ontology (GO) terms of these genes; the top 17 GO terms for these targets were related to functions in biological processes, biosynthetic processes, plastid, response to stress, regulation of biological processes, multicellular organismal development, response to abiotic stimuli, reproduction, protein binding, metabolic process, nucleus, catalytic activity, plasma membrane, binding, response to endogenous stimulus, anatomical structure morphogenesis and catabolic process (**Supplementary Fig. S89C**).

In addition to interactions between mRNAs and miRNAs, we also search for potential miRNA targets in the set of undefined transcripts. The undefined transcripts of *M. polymorpha* (29,627 contigs) were blasted against 669,430 lncRNA reference sequences (e^{-10}) in the NONCODE database (www.noncode.org). A total of 19 contigs of *M. polymorpha* contained lncRNAs that were homologous to the reference sequence of Arabidopsis, and one of them (LW225) was targeted by Mpo-miR11704.1. Thus, miRNAs also regulate lncRNA expression (**Supplementary Table S1**). In addition, we identified another 77 undefined transcripts, which have no homologs in the NONCODE database targeted by miRNAs. The information will be useful for further investigations (**Supplementary Table S1**).

We incorporated miRNA/target and degradome information into a custom-made *M. polymorpha* transcriptome database to generate a ContigViews-miRNA database, which provides confirmed results for public searching. The sequences of 129 miRNAs and 249 targets (171 genes and 78 undefined transcripts) are listed in **Supplementary Table S1**. Details regarding the precursor structures, miRNA–target pairing, and degradome evidence can be accessed in **Supplementary Figs. S1–S88**.

Identification of gene silencing-related pathways

To characterize the miRNA machinery of *M. polymorpha*, we identified *M. polymorpha* orthologs of core components involved in the different RNA-mediated gene silencing pathways in Arabidopsis (**Table 2**). We found two Argonaute family members, Mp*AGO1* (LW1759) and Mp*AGO4* (LW8524) (**Table 2**). Regarding the *DCL* family, we identified Mp*DCL1* (LW6271), which showed high similarity to At*DCL1* (**Table 2**). Additional orthologous genes of flowering plant gene silencing components were found, including Mp*SGS3* (LW4624), Mp*DRB2* (LW1470), Mp*NRPB2a* (LW8690) and Mp*RDR6* (LW8437) (**Table 2**). We were unable to identify a *HEN1* ortholog in *M. polymorpha*. However, we were able to detect miRNA methylation using established protocols for β-elimination. Here, *A. thaliana* Columbia ecotype (Col-0) and transgenic Arabidopsis expressing the *P1/HC-Pro* gene (*P1/HC* plant) were used as controls for evaluation of miRNA methylation efficiency (**Fig. 3**). P1/HC-Pro is a viral suppressor, which represses HEN1 function in miRNA 3′-end 2′-*O*-methylation (Yu et al. 2006). In Col-0 plants, miR166 shows 21 nt after β-elimination, indicating that 3′-end 2′-*O*-methylation (**Fig. 3**). However, P1/HC-Pro inhibits 3′-end 2′-*O*-methylation of miRNA, resulting in 20 nt of miR166 after β-elimination in *P1/HC* plants (**Fig. 3**). According to our β-elimination assay results, *M. polymorpha* miRNAs are methylated in vivo (21 nt after β-elimination) (**Fig. 3**), suggesting that either an as yet unfound HEN1 or other RNA methyltransferases of *M. polymorpha* might be involved in miRNA 3′-end 2′-*O*-methylation.

Conserved miRNAs in *M. polymorpha*

We identified four conserved pre-miRNAs (pre-Mpo-miR166a, pre-Mpo-miR390, pre-Mpo-miR529c and pre-Mpo-miR171) with full-length hairpin structures in our transcriptome (**Fig. 4A**). In accordance with the general rule that the miRNA is typically more abundant than the miRNA* (Bartel 2004, Lai et al. 2004, Kim and Nam 2006), the numbers of read counts for mature Mpo-miR166a, Mpo-miR390 and Mpo-miR529c were higher than those observed for their corresponding miRNA* strands (**Fig. 4A**, panels i, ii and iii). However, regarding Mpo-miR171-3p, a lower read count (10 reads) was observed for the miRNA than for Mpo-miR171-3p* (36 reads) (**Fig. 4A**, panel iv). Similar to pre-Ath-miR171, which produces Ath-miR171-5p and Ath-miR171-3p from both sides, the opposite side of Mpo-miR171-3p can produce another novel miRNA (Mpo-miR171-5p.2), which is predicted to target Mp*PHOT* (LW771; AB938188), which encodes a blue light photoreceptor phototropin in *M. polymorpha* (**Fig. 4A**, panel iv; **Supplementary Table S2**) (Komatsu et al. 2014). Additionally, pre-Mpo-miR529c can produce three isoforms, Mpo-miR529c.1 (5504 reads), Mpo-miR529c.2 (96 reads) and Mpo-miR529c.3 (133 reads), which target five different transcripts (**Fig. 4A**, panel iii).

MiRNAs corresponding to all four conserved pre-miRNAs can be detected in Tak1 and Tak2 accessions, and the Northern signals correlated with the deep sequencing read counts (**Fig. 4B**). We identified the targets of these four miRNAs by demonstrating evidence of miRNA-mediated cleavage (**Fig. 4C, D**). Mpo-miR166a targets the *CLASS III HOMEODOMAIN LEUCINE ZIPPER1* gene (Mp*C3HDZ1*; LW6010) (56 degradome reads at the 10th and 11th positions of the cleavage site) (**Fig. 4C**, panel i; **Fig. 4D**, panel i; **Table 3**) (Floyd and Bowman 2004), and Mpo-miR390 targets a *LEUCYL AMINOPEPTIDASE2* (AT4G30920) homolog-LW5937 in *M. polymorpha* (48 degradome reads at the cleavage sites) (**Fig. 4C**, panel ii; **Fig. 4D**, panel ii; **Table 3**). Notably, *TAS3*-like sequence has been found in *M. polymorpha* genomic DNA (Krasnikova et al. 2013); however, no miR390-targeted *TAS3* transcript was found in this study.

Table 2 List of genes related to transcriptional and post-transcriptional gene silencing and RNA-dependent DNA methylation in Arabidopsis and *Marchantia polymorpha*

Category	*A. thaliana* gene name	AGI number	Description	*M. polymorpha* contig ID	*M. polymorpha* gene name
ARGONAUTE	*AGO1*	AT1G48410	ARGONAUTE 1	LW1759	Mp*AGO1*
	AGO4	AT2G27040	ARGONAUTE 4	LW8524	Mp*AGO4*
DICER-like	*DCL1*	AT1G01040	DICER-LIKE 1	LW6271	Mp*DCL1*
HEN1	*HEN1*	AT4G20910	HUA ENHANCER 1	NA[a]	NA
SGS3	*SGS3*	AT5G23570	SUPPRESSOR OF GENE SILENCING 3	LW4624	Mp*SGS3*
DsRNA-binding protein	*DRB2*	AT2G28380	DsRNA-binding protein	LW1470	Mp*DRB2*
RNA polymerase	*NRPD2A*	AT3G23780	Nuclear RNA polymerase	LW8690	Mp*NRPD2A*
	RDR6	AT3G49500	RNA-dependent RNA polymerase	LW8437	Mp*RDR6*

[a] NA, not available.

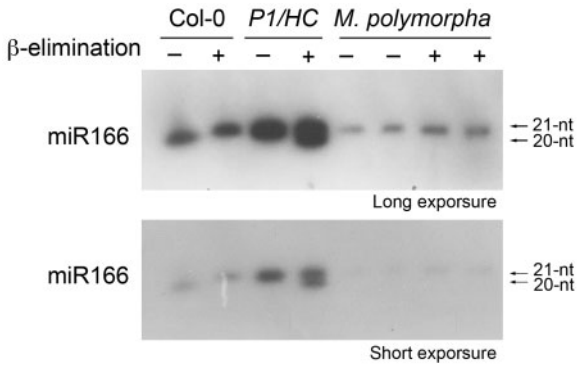

Fig. 3 Detection of miRNA 3′-end 2′-*O*-methylation in *Marchantia polymorpha*. β-Elimination assay of miR166 in Col-0, transgenic Arabidopsis expressing the *P1/HC-Pro* gene (*P1/HC*), and *M. polymorpha*. The upper panel shows an X-ray film after a long exposure (12 h). The lower panel shows an X-ray film after a short exposure (4 h).

Mpo-miR529c.1 targets LW1323 (112 degradome reads) and the *ENOYL-COA HYDRATASE2* (AT4G16210) homolog-LW7434 (102 degradome reads). Mpo-miR529c.2 targets the *MYB* TF (AT5G56110) homolog-LW8291 (17 degradome reads) and the homeodomain TF (AT2G40260) homolog-LW2562 (13 degradome reads), whereas Mpo-miR529c.3 targets the translation initiation factor (AT1G76810) homolog-LW2626 (16 degradome reads) (**Fig. 4C**, panels iii, and iv; **Fig. 4D**, panels iii and iv; **Table 3**). Mpo-miR171-3p targets a *GRAS* TF (AT1G66350) homolog-LW1838 in *M. polymorpha* (19 degradome reads) (**Fig. 4C**, panel v; **Fig. 4D**, panel v; **Table 3**). All of the conserved miRNAs and their target genes are listed in **Table 3**.

Conserved miRNAs without identified precursors

We also identified three conserved miRNA sequences (Mpo-miR408a, Mpo-miR160 and Mpo-miR319a) from small RNA profiles, but we did not identify their precursor sequences in the transcriptome database (**Table 3**), possibly because of low expression in the tissues analyzed or potential instability of the pre-miRNAs. Mpo-miR408a has two isoforms (Mpo-miR408a.1 and Mpo-miR408a.2) and 22 targets with significant degradome peaks (**Table 3**; **Supplementary Figs. S7–S28**). Mpo-miR160 targets an Mp*ARF3* (AB981319 in DDBJ; LW1641 in ContigViews) in *M. polymorpha* (**Table 3**; **Supplementary Fig. S1**) (Kato et al. 2015, Flores-Sandoval et al. 2016), whereas Mpo-miR319a targets the *MYB* TF (AT5G06100) homolog-LW575 (**Table 3**; **Supplementary Figs. S4, S5**).

MiRNAs control diverse plant processes

We identified the potential targets of 118 novel miRNAs by using degradome evidence (**Supplementary Table S1**; **Supplementary Figs. S30–S88**). Several developmental genes and stress response genes are controlled by Mp*MIR* genes. Regarding TF genes, Mpo-miR11671.1 targets the *SQUAMOSA PROMOTER BINDING PROTEIN-LIKE* (At*SPL*; AT1G02065) homolog-LW2610. Mpo-miR11693a and Mpo-miR11693b target another homeodomain TF (AT2G33550) homolog-LW6737. *SENSITIVE TO PROTON RHIZOTOXICITY1* (At*STOP1*; AT1G34370) TF homolog-LW1299 is targeted by Mpo-miR11677 (**Supplementary Tables S1, S2**). The other miRNA-targeted TF genes are listed in **Supplementary Table S2** and **Supplementary Fig. S91B**.

Regarding genes involved in nutrition pathways, Mpo-miR11690.1 targets the *LOW PHOSPHATE ROOT 1* (AT1G23010) homolog-LW5218, and Mpo-miR11683 targets the *SENSITIVE TO NITROGEN MUSTARD 1* (AT3G26680) homolog-LW17800. Moreover, Mpo-miR11678.2 targets the *PHOSPHATE TRANSPORTER 2;1* (At*PHT2;1*; AT3G26570) homolog-LW4390 (**Supplementary Tables S1, S2**). AtPHT2;1 is a shoot-specific low-affinity Pi transporter that was hypothesized to play a role in Pi loading of shoots (Daram et al. 1999).

Several *LEUCINE-RICH REPEAT* (*LRR*) genes, LW8529, LW2020 and LW7304, are targeted by Mpo-miR11680a.1, Mpo-miR11687.1 and Mpo-miR11674.1, respectively (**Supplementary Tables S1, S2**). Regarding stress and defense responses genes, Mpo-miR11670.2 targets the *ACCELERATED CELL DEATH2* (At*ACD2*; AT4G37000) homolog-Mp*Rccr* (LW12064); Mpo-miR11670.4 targets the *RESPONSIVE TO DEHYDRATION21* (At*RD21*; AT1G47128) homolog-LW1066; and Mpo-miR11720 targets the stress-responsive gene (AT2G32500) homolog-LW1514 and the *ENHANCED DOWNY MILDEW2* (At*EDM2*; AT5G55390) homolog-LW16495, respectively.

Regarding developmental genes, Mpo-miR11687.1 targets the *BARELY ANY MERISTEM2* (AT3G49670)

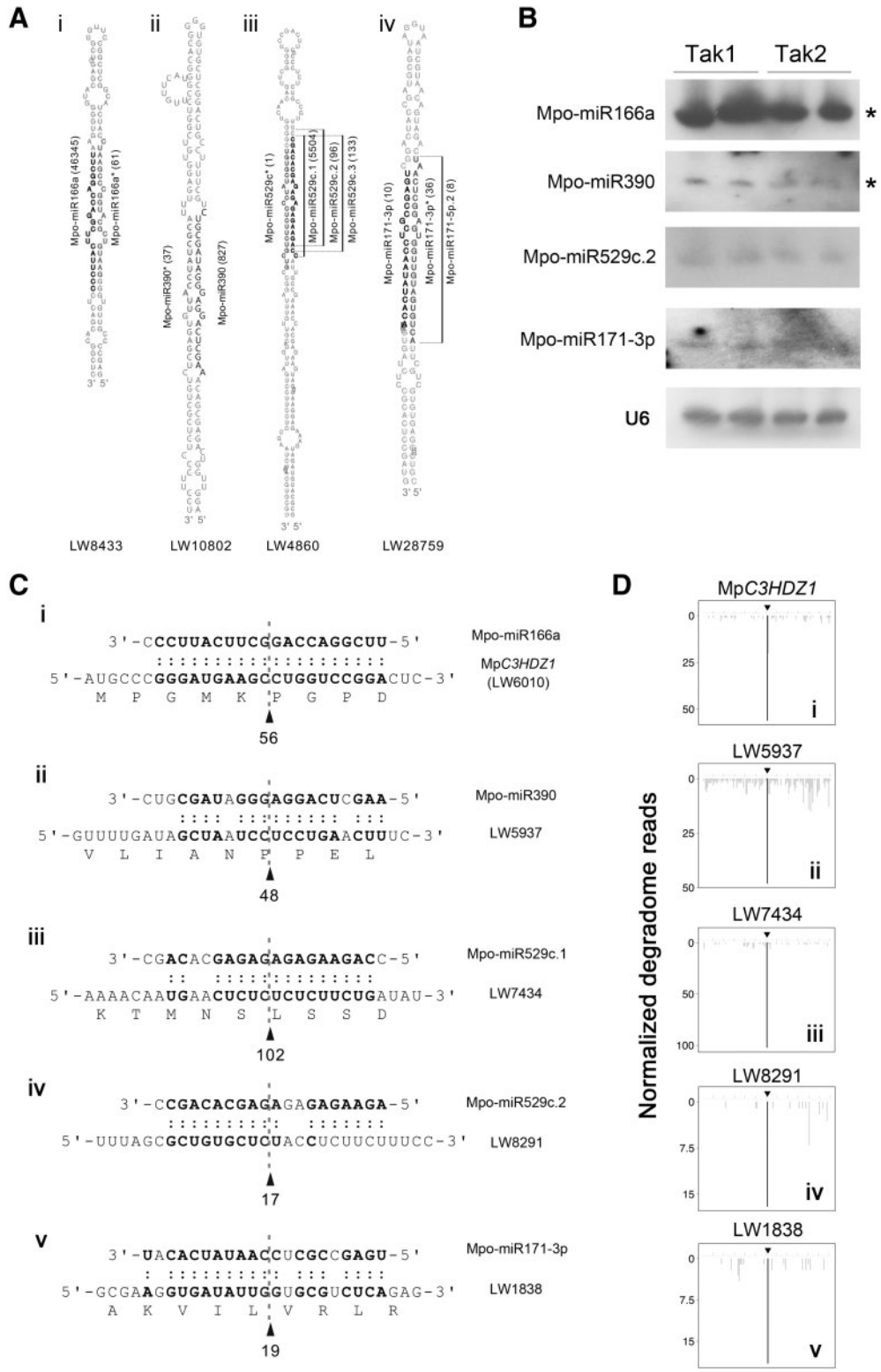

Fig. 4 Four conserved miRNAs in *Marchantia polymorpha*. (A) MiRNA precursor structures. Sequences in bold black represent miRNAs, while sequences in bold gray represent the miRNA* strands. Read counts are indicated in parentheses. (B) The detection of conserved miRNAs by Northern blot in *M. polymorpha*. U6 was used as a loading control. The asterisk indicates that the deep sequence of the small RNA comprises >700 read counts. (C) Conserved miRNAs and their pairwise target regions. The dashed line indicates the 10th and 11th positions of the miRNA. The arrowhead and the number indicate the position observed in the degradome and the number of read counts, respectively. (D) Degradome map of the miRNA target. The black line indicates significant (binomial test, *P*-value < 0.001) degradome read counts at the 10th and 11th positions of the target site. Degradome reads were normalized to the total degradome read counts.

Table 3 Function of genes targeted by conserved miRNAs

Target ID	Target name	Homolog AGI/EMBL	Function	miRNA	Precursor ID
LW6010	Mp*C3HDZ1*	AT1G52150	Homeobox-leucine zipper family	Mpo-miR166a	LW8433
LW5937	NA	AT4G30920	Leucine aminopeptidase chloroplastic-like	Mpo-miR390	LW10802
LW5678	NA	AT2G39260	RNA binding		
LW1323	NA	CAN66130	NA[a]	Mpo-miR529c.1	LW4860
LW7434	NA	AT4G16210	Enoyl-CoA hydratase/isomerase A		
LW8291	NA	AT5G56110	R2R3 MYB transcription factor	Mpo-miR529c.2	
LW2562	NA	AT2G40260	Homeodomain-like superfamily		
LW2626	NA	AT1G76810	Translation initiation factor	Mpo-miR529c.3	
LW1838	NA	AT1G66350	Negative regulator of gibberellin responses	Mpo-miR171-3p	LW28759
LW11608	NA	AT5G07475	Cupredoxin superfamily protein	Mpo-miR408a.1	NA
LW12208	NA	AT2G25060	*EARLY NODULIN-LIKE PROTEIN 14*		
LW1579	NA	AT1G76100	*PLASTOCYANIN 1*		
LW1761	NA	AT3G17810	*PYRIMIDINE 1*		
LW1935	NA	EDQ69569	NA		
LW2509	NA	AT5G11840	NA		
LW2886	NA	AT5G49800	Polyketide cyclase/dehydrase and lipid transport superfamily protein		
LW3258	NA	AT5G49580	Chaperone DnaJ-domain superfamily protein		
LW3469	NA	EDQ61308	NA		
LW3745	NA	AT4G14420	HR-like lesion-inducing protein-related		
LW3787	NA	ABK21292	NA		
LW3821	NA	AT2G40690	*SUPPRESSOR OF FATTY ACID DESATURASE DEFICIENCY 1*		
LW4132	NA	AT2G42520	P-loop-containing nucleoside triphosphate hydrolases superfamily protein		
LW5963	NA	AT1G69060	Chaperone DnaJ-domain superfamily protein		
LW6869	NA	AT5G21105	L-Ascorbate oxidase		
LW8835	NA	AT3G60810	NA		
LW8846	NA	AT2G02850	*PLANTACYANIN*		
LW17444	NA	AT3G17910	*EMBRYO DEFECTIVE 3121*		
LW3186	NA	AT5G06000	*EUKARYOTIC TRANSLATION INITIATION FACTOR 3G2*		
LW8164	NA	EBG08682	NA		
LW13438	NA	AT3G16110	*PROTEIN DISULFIDE ISOMERASE 4*	Mpo-miR408a.2	
LW4001	NA	AT5G02160	NA		
LW1641	Mp*ARF3*	AT2G28350	*AUXIN RESPONSE FACTOR 10*	Mpo-miR160	NA
LW3585	NA	AT1G18790	*RWP-RK DOMAIN-CONTAINING 1*	Mpo-miR319a	NA
LW575	NA	AT5G06100	*MYB DOMAIN PROTEIN 33*		

[a] NA, not available.

homolog-LW2536, Mpo-miR11679.1 targets the *VERNALIZATION INDEPENDENCE4* (At*VIP4*; AT5G61150) homolog-LW4639, and Mpo-miR11718.1 targets the *GRF1-INTERACTING FACTOR3* (AT4G00850) homolog-LW4216. Finally, Mpo-miR11704.2 targets the *HISTONE 3.3* (AT5G10980) homolog-LW1290. Detailed information is provided in **Supplementary Tables S1** and **S2**, and **Supplementary Figs. S1–S88**.

Novel miRNAs regulate Mp*AGO1* and Mp*MADS* genes in *M. polymorpha*

We highlight 15 novel miRNAs (Mpo-miR11685.1, Mpo-miR11681.1, Mpo-miR11671.1, Mpo-miR11680a.1, Mpo-miR11687.1, Mpo-miR11677.1, Mpo-miR11698.1, Mpo-miR11670.2, Mpo-miR11707.1, Mpo-miR11707.2, Mpo-miR11692.1, Mpo-miR11676, Mpo-miR11669.1, Mpo-miR11672.2 and Mpo-miR11668), which have important targets in *M. polymorpha*, as their respective Arabidopsis homologs exert crucial functions in developmental processes (**Table 4**). As shown in **Fig. 5**, two miRNA precursors, pre-Mpo-miR11687.1 and pre-Mpo-miR11681, can generate two novel miRNAs. However, pre-Mpo-miR11707 can generate two miRNAs, Mpo-miR11707.1 and Mpo-miR11707.2, from the stem–loop (**Fig. 5A**, panel i). Our data show that both miRNAs can target Mp*AGO1* (LW1759) mRNA (**Fig. 5B**, panels i, and ii). Mpo-miR11707.1, the major 21 nt species (1,654 read counts from small RNA profiles) can also be detected in *M. polymorpha* Tak1 and Tak2 accessions by Northern blot (**Fig. 5C**). Moreover, the degradome profile also shows a significant degradome peak (76 degradome reads; $P < 0.01$) at the

Table 4 Function of genes targeted by novel miRNAs

Target ID	Target name	Homolog AGI/EMBL	Function	miRNA	Precursor ID
LW4492	NA[a]	AT4G14465	AT-hook motif nuclear-localized 20	Mpo-miR11685.1	LW2962
LW14289	Mp*MADS2*	EDQ77973	MIKC^C MADS domain	Mpo-miR11681.1	LW11075
LW7948	NA	AT5G50840	NA		
LW6190	NA	EFJ17613	NA		
LW8165	NA	AT3G27820	Peroxisome membrane-bound monodehydroascorbate reductase		
LW22348	NA	EFJ28954	NA		
LW7577	NA	AT5G54310	ARF GAP domain	Mpo-miR11681.2	
LW2610	NA	AT1G02065	*SQUAMOSA PROMOTER BINDING PROTEIN-LIKE 8*	Mpo-miR11671.1	LW14438
LW14116	NA	EAZ44452	NA	Mpo-miR11680a.1	LW22799
LW5512	NA	AT3G46640	LUX ARRHYTHMO		
LW3805	NA	AT3G44200	NIMA-related serine/threonine kinase		
LW8529	NA	AT2G30105	NA		
LW2328	Mp*MADS1*	AT1G22130	MIKC* MADS domain	Mpo-miR11687.1	LW20753
LW2536	NA	AT3G49670	*BARELY ANY MERISTEM 2*		
LW2020	NA	AT1G75640	Leucine-rich receptor-like protein kinase		
LW10506	NA	EFJ06590	NA		
LW3476	NA	AT3G61050	*CALCIUM-DEPENDENT LIPID-BINDING PROTEIN*		
LW921	NA	AT1G30450	*CATION-CHLORIDE CO-TRANSPORTER 1*	Mpo-miR11677	LW11685
LW9386	NA	AT1G48380	*HYPOCOTYL 7*		
LW28862	NA	EFJ23241	NA		
LW798	NA	AT2G27290	NA		
LW8919	NA	AT2G20780	Carbohydrate transmembrane transporter activity		
LW3390	NA	AT1G55350	*DEFECTIVE KERNEL 1*		
LW2282	NA	AT4G38160	*PIGMENT DEFECTIVE 191*		
LW3379	NA	AT1G75200	Radical SAM domain-containing protein		
LW769	NA	AT5G47390	*MYB HYPOCOTYL ELONGATION-RELATED*	Mpo-miR11698.1	LW2397
LW5196	NA	AT5G41950	Tetratricopeptide repeat (TPR)-like superfamily		
LW3777	NA	AT1G75350	*EMBRYO DEFECTIVE 2184*	Mpo-miR11670.2	LW5243
LW12064	Mp*Rccr*	AT4G37000	*ACCELERATED CELL DEATH 2*		
LW1759	Mp*AGO1*	AT1G48410	*ARGONAUTE 1*	Mpo-miR11707.1	LW2038
LW1946	NA	AT1G02080	Transcription regulator activity		
LW1759	Mp*AGO1*	AT1G48410	*ARGONAUTE 1*	Mpo-miR11707.2	LW2038
LW9825	Mp*PPR_66*	AT2G17033	Pentatricopeptide repeat-containing protein	Mpo-miR11692.1	LW9825
LW573	NA	AT5G57420	*INDOLE-3-ACETIC ACID-INDUCIBLE 33*		
LW1753	NA	EDQ70928	NA	Mpo-miR11669.1 Mpo-miR11672.2 Mpo-miR11668	LW13964 LW327 LW6532

[a] NA, not available.

10th and 11th positions of the target site (**Fig. 5D**, panel i). Mpo-miR11707.2 (22 nt) is less abundant with only 48 read counts, and also shows a significant degradome peak ($P < 0.01$), although the peak only has 18 degradome reads (**Fig. 5D**, panel ii). Our data provide evidence of Mpo-miR11707.1- and Mpo-miR11707.2-mediated Mp*AGO1* cleavage.

Mpo-miR11687.1 and Mpo-miR11681.1 target two MADS-box genes, Mp*MADS1* (LW2328) and Mp*MADS2* (LW14289) (**Table 4**; **Fig. 5A**, panels ii and iii; **Fig. 5B**, panels iii and iv), and generate 396 and 321 degradome read counts, respectively (**Fig. 5D**, panels iii and iv). In addition, Mpo-miR11687.1 can be detected by Northern blot in *M. polymorpha* (**Fig. 5C**), further supporting an in planta activity. Notably, most of the *M. polymorpha* miRNAs, which have >700 read counts in small RNA profiles, can be detected by Northern blot (**Figs. 4**, **5**; **Supplementary Fig. S90**).

Reporter assay to confirm miRNA-mediated target down-regulation

Next, we used reporter assays to evaluate the down-regulation of Mp*C3HDZ1*, Mp*AGO1* and Mp*MADS1/2* expression when Mpo-miR166a, Mpo-miR11707.1, Mpo-miR11687.1 and Mpo-miR11681.1 were co-expressed in *Nicotiana benthamiana* (**Fig. 6**). A 120 nt DNA fragment, which contained the miRNA

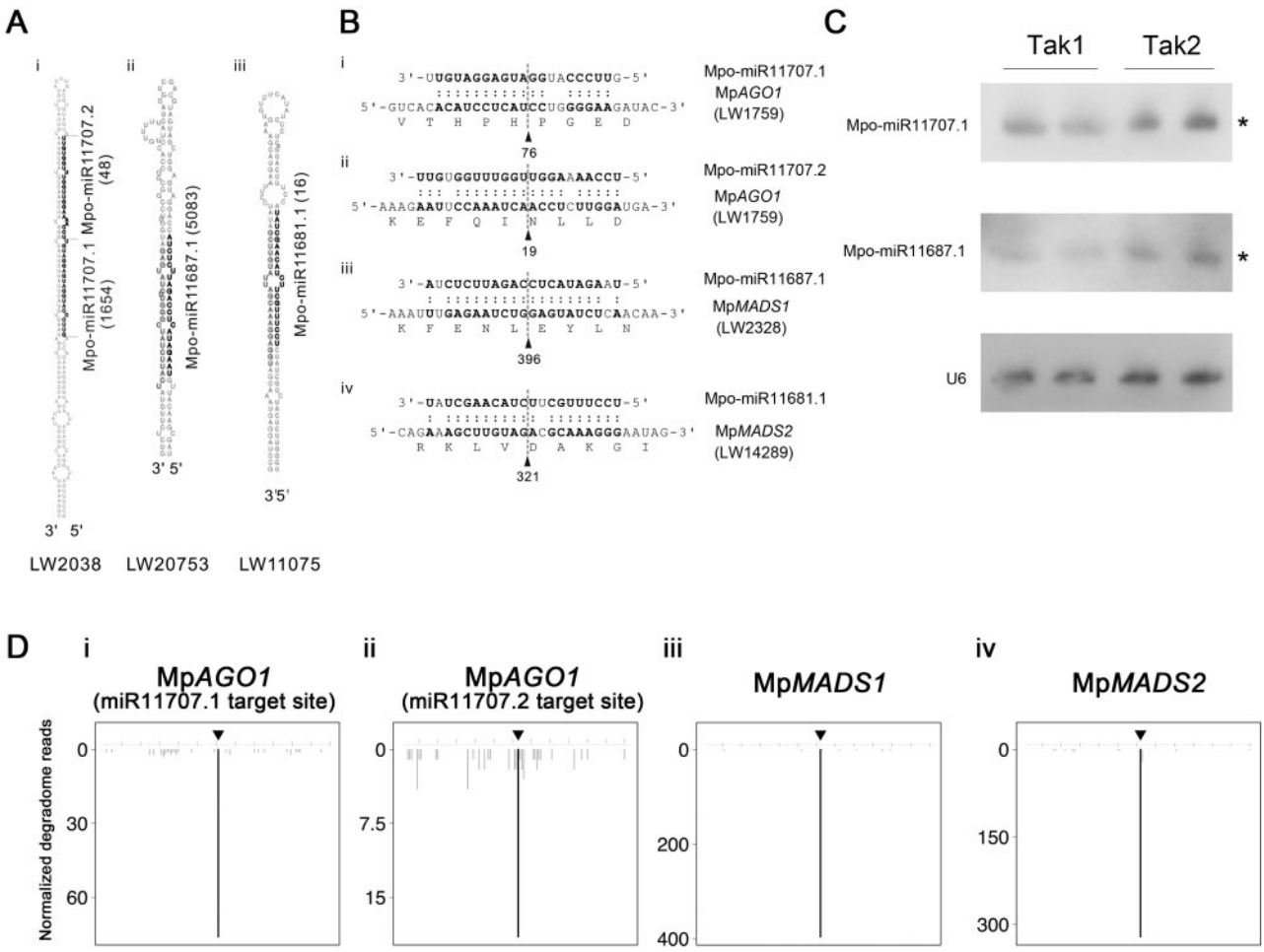

Fig. 5 Four novel miRNAs that regulate *AGO1* and *MADS* genes in *Marchantia polymorpha*. (A) Four novel miRNA precursor structures. Sequences in bold black represent miRNAs, while sequences in bold gray represent miRNA* strands. Read counts are indicated in parentheses. (B) Four novel miRNAs and their pairwise target regions. The dashed line indicates the 10th and 11th positions of the miRNA. The arrowhead and the number indicate the position observed in the degradome and the number of read counts, respectively. (C) The detection of novel miRNAs by Northern blot in *M. polymorpha*. U6 was used as a loading control. The asterisk indicates that the miRNA sequence comprises >700 read counts. (D) Degradome map of the miRNA target. The black line indicates the significant (binomial test, *P*-value < 0.001) degradome read counts at the 10th and 11th positions of the target site.

target site for each gene, was fused to the 5′ end of the *YFP* (yellow fluorescent protein) gene and the chimeric construct was expressed in a binary vector under the control the 35S promoter. A construct expressing only *YFP*, without Mpo-miR166a, was used as a negative control. The data indicate that YFP expression was not significantly affected by the presence of Mpo-miR166a in the chimeric construct (**Fig. 6B, C**, panel i). Notably, endogenous miR166 was detected in *N. benthamiana* tissues lacking Mpo-miR166a, but at low levels compared with those in tissues co-expressing Mpo-miR166a (**Fig. 6C**, panels i and ii). Interestingly, the construct, Mp*C3HDZ1-YFP*, which contains a wild-type miR166 target site (**Fig. 6A**, panel ii), showed either no YFP signal or low RNA accumulation in tissues, regardless of whether Mpo-miR166a was present or absent (**Fig. 6B, C**, panel ii). However, the miR166-resistant mutant Mp*C3HDZ1*^{mut}*-YFP* (**Fig. 6A**, panel iii) exhibited a high YFP signal and a high level of mRNA accumulation in tissues where Mpo-miR166a was absent (**Fig. 6B, C**, panel ii). The YFP signal of Mp*C3HDZ1*^{mut}*-YFP* was reduced in Mpo-miR166a-expressing tissues, suggesting that overexpression of Mpo-miR166a can still cleave the mutated site (three mismatches) to some extent. In summary, pre-Mpo-miR166a can be processed into Mpo-miR166a by the machinery of *N. benthamiana* plants and Mpo-miR166a is able to down-regulate Mp*C3HDZ1*.

Co-expression of the Mp*AGO1-YFP* construct with Mpo-miR11707.1 in *N. benthamiana* leaf cells led to a reduction in YFP fluorescence compared with the Mp*AGO1-YFP*-only sample (**Fig. 6B**). In addition, the real-time reverse transcription–PCR (RT–PCR) results also showed a reduction in the Mp*AGO1-YFP* signal when Mpo-miR11707.1 was present (**Fig. 6C**, panel iii). Similarly, the Mp*MADS1-YFP* construct also shows a reduced YFP signal when it was co-expressed with Mpo-miR11687.1 (**Fig. 6B, D**, panel i). In contrast, the Mpo-miR11687.1-resistant mutant (Mp*MADS1*^{mut}*-YFP*) did not show reduced mRNA levels when Mpo-miR11687.1 was co-expressed (**Fig. 6D**, panel ii). A similar result was also observed when Mp*MADS2-YFP* constructs were co-expressed

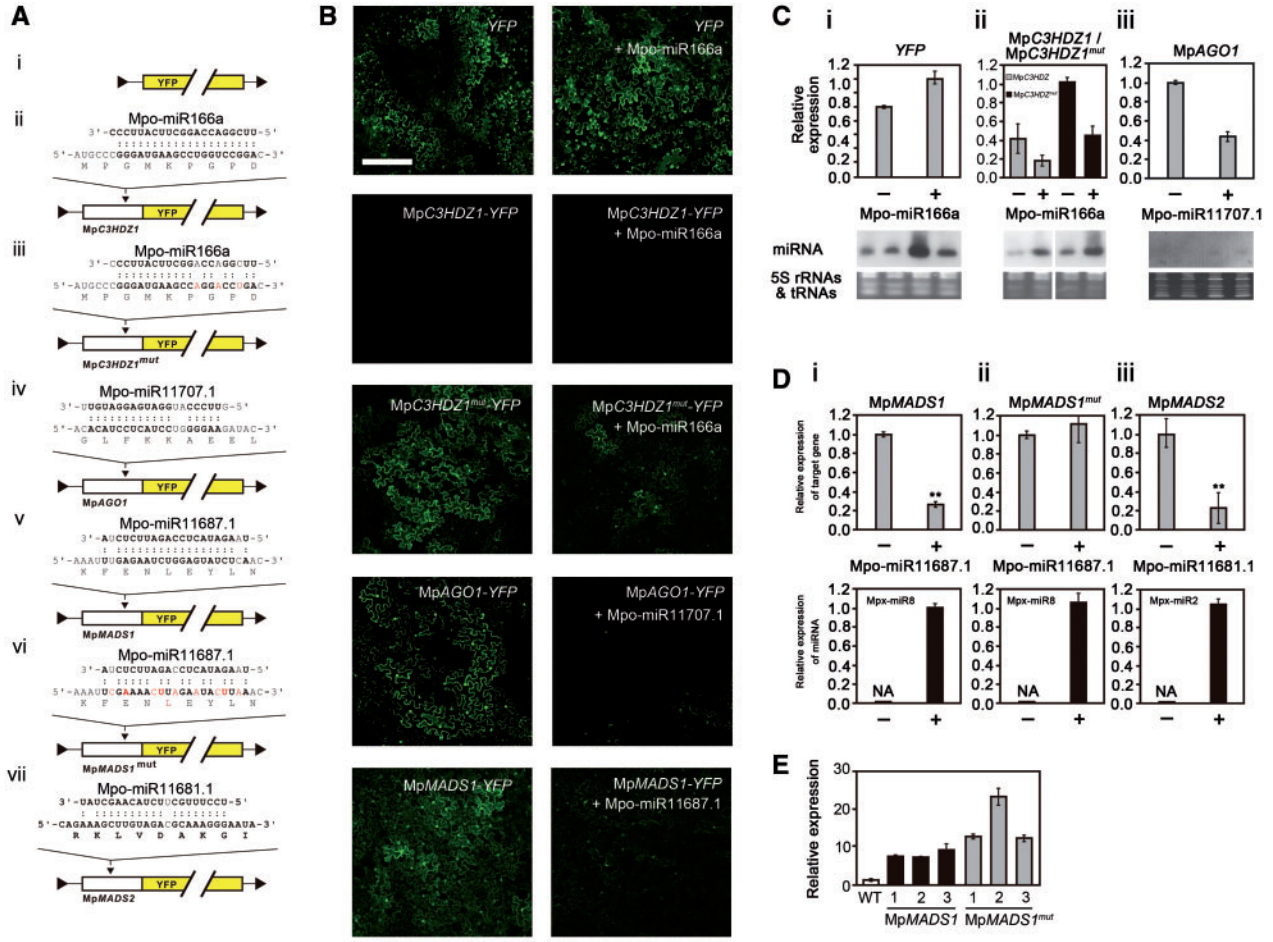

Fig. 6 Reporter assay conducted to monitor the miRNA-mediated down-regulation of predicted targets by transient expression in *Nicotiana benthamiana*. (A) Schematic of miRNAs pairing with their target sites on the *YFP* fusion constructs. The red nucleotides are mutated target site nucleotides. All of the genes were cloned into a binary vector under the control of the 35S promoter. A *YFP*-only construct (i) was used as a negative control. The Mp*C3HDZ1-YFP* (ii), Mp*C3HDZ1*^{mut}*-YFP* (iii), Mp*AGO1-YFP* (iv), Mp*MADS1-YFP* (v), Mp*MADS1*^{mut}*-YFP* (vi) and Mp*MADS2-YFP* (vii) contructs contain 120 nt of the 5′ end of the gene; thus, they contain the Mpo-miR166a, Mpo-miR11707.1, Mpo-miR11687.1 and Mpo-miR11681.1 target sites, respectively, fused with the *YFP* gene. (B) YFP reporter assays were assessed using confocal microscopy. Scale bar = 250 μm. (C) The relative expression of the *YFP* reporter with/without miRNAs. The miRNAs were detected by Northern blot. 5S rRNA and tRNAs were used as loading controls. (D) The relative expression of Mp*MADS-YFP* genes with/without miRNAs. The miRNAs were detected by stem–loop real-time RT–PCR, and miRNA levels were normalized to endogenous miR159 expression in *N. benthamiana*. Relative expression of the targets was normalized to the expression of Nb*Actin* as assessed by real-time RT–PCR. Bars represent the SEs ($n = 3$). The relative expression of the target in the presence of a miRNA precursor is significantly different from that in the presence of the target only (without miRNA treatment) for each RNA sample, according to the results of Student's *t*-test; $^{*}P < 0.05$; $^{**}P < 0.01$. (E) Relative expression of wild-type Mp*MADS1* and the mutagenized miRNA-resistant Mp*MADS1*^{mut} in *pro*Mp*EF1α*:Mp*MADS1* and *pro*Mp*EF1α*:Mp*MADS1*^{mut} *M. polymorpha* plants, respectively. Mp*MADS1* expression in *M. polymorpha* transformed with an empty vector was set to '1' and served as the wild-type (WT) reference. The numbers below indicate three independent transgenic *M. polymorpha* lines. Bars indicate the mean ± SE ($n = 3$).

with Mpo-miR11681.1 (**Fig. 6D**, panel iii). Transient Mpo-miR11687.1 and Mpo-miR11681.1 expression was detected by real-time RT–PCR (**Fig. 6D**, lower panels).

Moreover, the miRNA-resistant versions of Mp*MADS1*^{mut} and Mp*MADS1* genes were expressed under the control of the strong *M. polymorpha elongation factor promoter 1α* (Mp*EF1α*) (Althoff et al. 2014) in *M. polymorpha*. Transgenic plants overexpressing Mp*MADS1*^{mut} showed a 12- to 24-fold increase of miRNA-resistant Mp*MADS1*^{mut} mRNA expression compared with endogenous Mp*MADS1* expression, whereas overexpression of Mp*MADS1* caused only a 7- to 9-fold increase in expression (**Fig. 6E**). Expression of the miRNA-resistant Mp*MADS1*^{mut} thus led to an approximately 2-fold increase in the accumulation of Mp*MADS1*^{mut} mRNA in transgenic *M. polymorpha* plants, supporting the ability of Mpo-miR11687.1 to target Mp*MADS1* in planta (**Fig. 6E**). Even though the miRNA-processing machinery in *M. polymorpha* and *N. benthamiana* might be functionally different, our data clearly show that *M. polymorpha* miRNAs can be processed in the *N. benthamiana* heterologous system and that these novel miRNAs are able to down-regulate their targets in vivo. Further evaluation of such miRNA/target circuits in *M. polymorpha* might reveal the uniqueness of the miRNA pathway in these distant species. Data from additional reporter assays aiming to

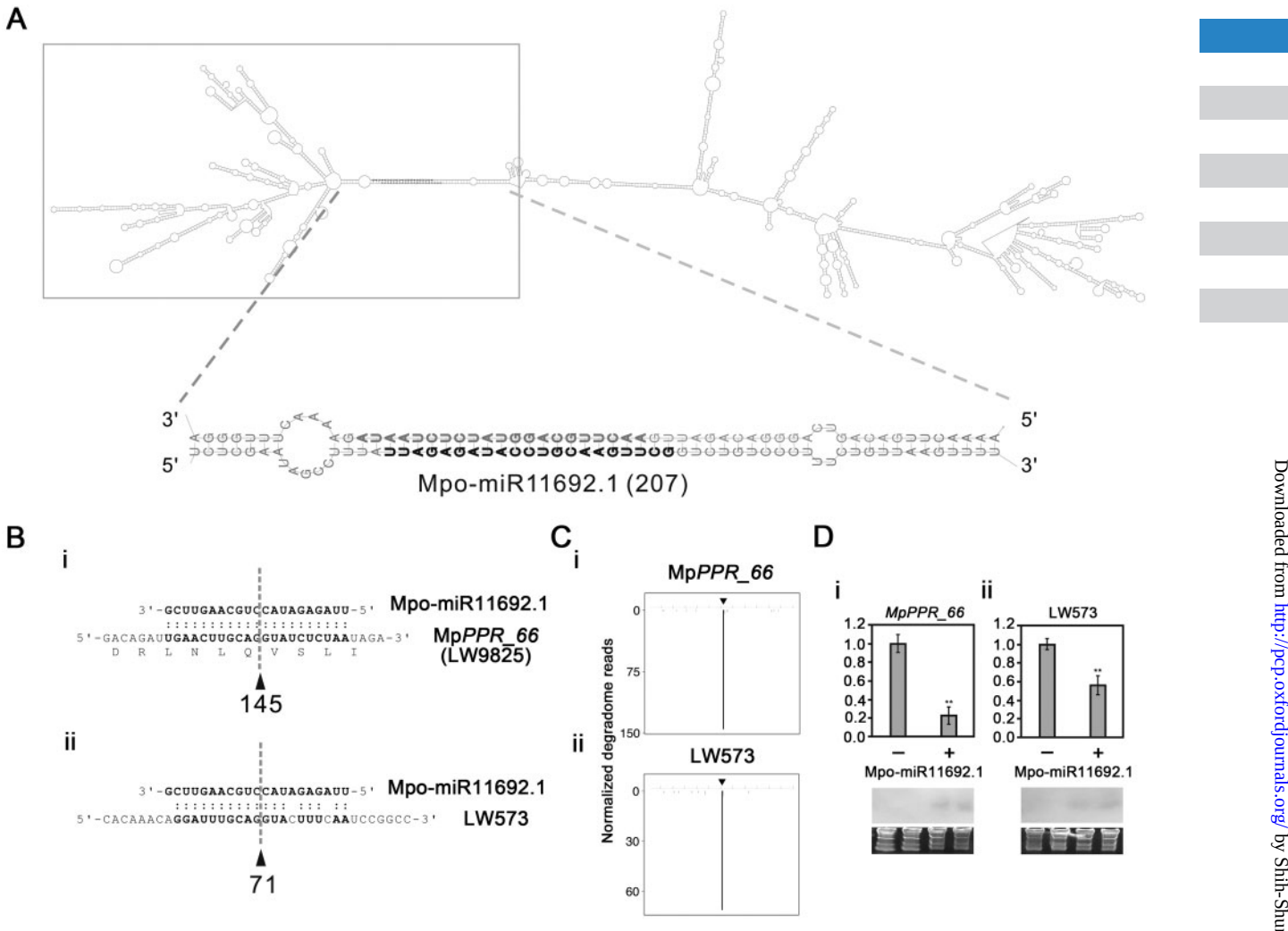

Fig. 7 The Mp*PPR_66* (LW9825) transcript generates Mpo-miR11692.1 to target its mRNA and other targets. (A) The secondary structure of the Mp*PPR_66* transcript, and the hairpin structure for the generation of Mpx-miR15.1. (B) Paired regions of Mpo-miR11692.1/Mp*PPR_66* (i) and Mpo-miR11692.1/LW573 (ii). The dashed line indicates the 10th and 11th positions of the miRNA. The arrowhead and number indicate the position observed in the degradome and the number of read counts, respectively. (C) Degradome map of the miRNA target. The black line indicates significant (binomial test *P*-value < 0.001) degradome read counts at the 10th and 11th position of the target site. (D) Reporter assay to monitor Mpo-miR11692.1/Mp*PPR_66* (i) and Mpo-miR11692.1/LW573 (ii) interactions following transient expression in *Nicotiana benthamiana*. The relative expression of the targets was normalized to the expression of Nb*Actin* determined by real-time RT–PCR. Bars represent the SEs ($n = 3$). The relative expression of the targets in the presence of a miRNA precursor was significantly different from the expression in the presence of the target only (without miRNA treatment) for each RNA sample, according to the results of Student's *t*-test; $^{*}P < 0.05$; $^{**}P < 0.01$. The miRNAs were detected by Northern blot. 5S rRNA and tRNAs were used as loading controls.

evaluate additional targets and relationships among conserved/novel miRNAs are presented in **Supplementary Fig. S92**.

Role of long miRNA precursors in miRNA biogenesis and target regulation

Interestingly, we identified two precursors, pre-Mpo-miR11672 (LW327) and pre-Mpo-miR11670 (LW5243), which have long and complex structures (**Supplementary Figs. S33, S35**). Mpo-miR11670.2 targets the *EMBRYO DEFECTIVE 2184* (AT1G75350) homolog-LW3777 and the At*ACD2* homolog-LW12064 (**Table 4**; **Supplementary Fig. S33**). Mpo-miR11672.2 targets LW1753, a gene of unknown function (**Table 4**; **Supplementary Fig. S35**). Importantly, LW1753 is also targeted by Mpo-miR11668 and Mpo-miR11669.1, albeit at different positions (**Table 4**; **Supplementary Figs. S31, S32**).

In addition, the *PENTATRICOPEPTIDE REPEAT* gene transcript of *M. polymorpha* [Mp*PPR_66* (LW9825)] has a complex secondary structure (**Fig. 7A**). Its transcript has a stem–loop structure, and it can produce Mpo-miR11692.1 to target itself as well as the *INDOLE-3-ACETIC ACID INDUCIBLE* (AT5G57420) homolog-LW573 (**Fig. 7A, B**; **Table 4**). The read count of Mpo-miR11692.1 (207 reads) in *M. polymorpha* is too low to be detected by Northern blot (**Supplementary Fig. S90**); however, the degradome profiles showed 145 and 71 degradome reads at target sites of Mp*PPR_66* and LW573, respectively (**Fig. 7B, C**). In the reporter assay, Mpo-miR11692.1 was shown to down-regulate its precursor (Mp*PPR_66*) and LW573 (**Fig. 7D**).

Discussion

An integrated approach for characterizing *M. polymorpha* miRNAs

In this study, we integrated transcriptome, small RNA and degradome profiles using the ContigViews-miRNA platform to develop a pipeline for the prediction of *M. polymorpha* miRNAs and miRNA targets. This pipeline can be applied to predict miRNAs/targets in both model and non-model, organisms. Although the availability of a reference genome for the study of small RNAs is very useful, characterizing the small RNA component on a transcriptomic level is possible through a combination of RNA-Seq and degradome analyses. Notably, fast turnover rates of miRNAs might affect the results of miRNA prediction (Sanei and Chen 2015).

Transcriptome sequences represent the existing transcripts in a particular tissue of an organism at a specific physiological and developmental moment. Therefore, using transcriptomic sequences for miRNAs and precursor identification can exclude false-positive hairpin structures such as those predicted from genomic DNA. However, the draft of genomic DNA contigs in non-model organisms can help to rule out misassembled transcripts or short contig sequences, which might be unable to form a hairpin structure, to enhance the prediction accuracy. Moreover, integrating the degradome profile improves the accuracy of miRNA and target prediction.

MiRNA target prediction in plants can be performed with the aid of well-established software programs such as the psRNAtarget web server, which predicts hundreds of targets that are likely to be down-regulated by miRNA-mediated cleavage or translation inhibition (Dai and Zhao 2011). However, evaluating hundreds of predicted miRNA–target relationships one by one through an experimental approach is difficult. The RNA degradome is comprised of 5′-end sequences from degraded RNA that can be used to confirm the accuracy of such predictions. An assessment of degradome sequences allows miRNA-mediated cleavage (clear read accumulation peaks at the 10th and 11th positions of the target site) to be differentiated from mRNA decay (a widespread pattern of reads dispersed throughout the transcript). For example, we recently reported a degradome analysis showing that At-miR396 triggers decay of Arabidopsis *SHORT VEGETATIVE PHASE* mRNA by translation inhibition, resulting in multiple degradome peaks, showing that the degradome peaks are approximately 100 nt 3′ to the miR396 target site (Yang et al. 2015).

The first 5′-end nucleotide of miRNA is a major determinant for sorting the miRNA into a particular AGO complex. In Arabidopsis, AGO1 favors a 5′-terminal 'U', whereas AGO2 and AGO4 preferentially recruit a 5′-terminal 'A', and AGO5 perferentially binds a 5′-terminal 'C' (Mi et al. 2008). However, 5′-terminal 'G' exists at low levels in these AGOs in Arabidopsis. We observed several new features of *M. polymorpha* miRNAs and their targets. First, as reported in Arabidopsis, 46.5% of the first 5′-end nucleotides of miRNAs are 'U', which suggests a loading affinity for MpAGO1. Interestingly, 14.7% of Mpo-miRNAs (19 miRNAs) have a 'G' as the first 5′-end nucleotide. Thus, the presence of a first-G miRNA might be a feature of extant *M. polymorpha*. Secondly, the coding gene Mp*PPR_66* has a long stem–loop that can produce an Mpo-miR11692.1 to control its own mRNA and other mRNAs.

MiRNAs regulate defense/stress responses and chromatin remodeling

Through miRNA/target identification studies, numerous miRNA-regulated targets with homologs that are involved in stress responses and defense (e.g. At*ACD2*, At*RD21*, At*EDM2*, *LRRs* and heat shock proteins) were identified in *M. polymorpha*. In Arabidopsis, AtACD2 can either suppress mitochondrial oxidative bursts and protect cells or modulate cell death (Pattanayak et al. 2012). AtRD21 is a granulin domain-containing cysteine protease implicated in the stress response and defense (Lampl et al. 2013). AtEDM2 is required for RPP7-dependent disease resistance in Arabidopsis (Eulgem et al. 2007) and is a chromatin regulator that controls CHG methylation in the genome (Lei et al. 2014). The functions of these homologs imply that similar defense mechanisms exist in *M. polymorpha* and that these mechanisms are modulated by miRNAs.

A previous study demonstrated that At*STOP1* was involved in a signal transduction pathway associated with acid soil tolerance in Arabidopsis roots (Iuchi et al. 2007). However, Ppt-miR1023a, which is significantly differentially expressed during the juvenile to adult gametophyte stage transition, controls one At*STOP1* homolog in *P. patens* (Arazi 2012). Consistently, Mpo-miR11677 controls an At*STOP1* homolog in *M. polymorpha*. Moreover, At*VIP4* is involved in seed dormancy and is required for the expression of the flowering repressor *FLC* by modulating histone H3K36 methylation on the promoter region (Zhao et al. 2005, Liu et al. 2011). The *HISTONE 3.3* homolog is also regulated by Mpo-miR11704.2.

Across kingdoms, lncRNA transcripts function as modular scaffolds with higher order organization as part of ribonucleoprotein complexes that interact with numerous chromatin regulators to target specific genomic locations (Rinn and Chang 2012, Werner and Ruthenburg 2015). In plants, lncRNAs are involved in diverse developmental programs during vernalization, fertilization, photomorphogenesis, phosphate homeostasis, alternative splicing and protein re-localization (Campalans et al. 2004, Heo and Sung 2011, Ding et al. 2012, Jabnoune et al. 2013, Bardou et al. 2014, Wang et al. 2014). Here, we demonstrated that 78 undefined transcripts were cleaved by 37 miRNAs in *M. polymorpha*. To determine the nature of these transcripts, whether non-coding or otherwise, will require a comprehensive annotation of the *M. polymorpha* genome. In addition, these Mp*MIR* genes and targets are good candidates for use in studies of gametophyte and sporophyte phase transitions in the future.

Evolution of land plant miRNAs

To place our findings in perspective, we first compared the set of miRNAs identified in *M. polymorpha* with those found in species of the other major lineages of land plants. Restricting comparisons to those miRNAs found in more than one of the

lineages represented by genome sequences (seed plants, lycophytes and mosses), we found that among the 10 miRNAs that are conserved between *Physcomitrella* and either *Selaginella* or seed plants, seven also exist in *M. polymorpha* (**Table 5**). Thus, these seven miRNAs are probably evolved from a common ancestor of extant land plants.

Two of the conserved miRNAs target orthologous genes found throughout land plants. In Arabidopsis, *C3HDZ* transcripts are regulated by Ath-miR165/166 (Emery et al. 2003, Mallory et al. 2004). Mpo-miR166a, the most abundant Mpo-miRNA in vivo in our samples, regulates the orthologous *M. polymorpha* gene Mp*C3HDZ1* (Floyd and Bowman 2004). *C3HDZ* genes encode plant-specific TFs involved primarily in shoot development (McConnell et al. 2001, Emery et al. 2003, Floyd et al. 2006, Prigge and Clark 2006). Likewise, Mpo-miR160 regulates Mp*ARF3*, which is orthologous to the Arabidopsis *ARF* genes regulated by Ath-miR160 (Flores-Sandoval et al. 2016). These examples demonstrate that miRNAs and their targets may be conserved over a considerable length of evolutionary time. Perhaps of more interest are conserved miRNAs that do not have orthologous targets. However, for at least two conserved miRNAs (miR171 and miR529), the conserved miRNA may target homologs, suggesting that a more complex evolution, perhaps in the form of gene loss and loss of miRNA regulation, could explain their target relationships in disparate land plants.

We also compared the miRNAs identified in *M. polymorpha* with those identified in *P. endiviifolia* (Alaba et al. 2015). Remarkably, of the miRNAs identified in the two liverwort species that are not conserved across land plants, no overlap was detected, suggesting that the vast majority of miRNAs are lineage specific within liverwort species. While this may appear surprising, the last common ancestor of *Marchantia* and *Pellia* probably pre-dated the Permian; thus the two species have followed independent trajectories for an extended period of time (Walton 1925, Anderson 1976, Feldberg et al. 2014).

Our data contribute to the idea that the majority of miRNA families identified thus far in different plant species are highly lineage specific. For example, approximately 70% of known Arabidopsis miRNA families lack apparent homologs outside of Brassicaceae (Rajagopalan et al. 2006, Fahlgren et al. 2007, Fahlgren et al. 2010, Ma et al. 2010). According to an analysis of miRNAs in monocots, moss and lycopods (Axtell et al. 2007, Lu et al. 2008), these lineages also possess large numbers of miRNA families that are not broadly conserved and thus are not derived from a last common ancestor. Likewise, miRNAs unique to the closely related Arabidopsis species *A. thaliana* or *A. lyrata* tend not to be found in a third species, *Capsella rubella* (Fahlgren et al. 2010). Together, these differences in miRNAs among close plant relatives support the notion that plant miRNA evolution is highly dynamic. Most non-conserved *M. polymorpha* miRNAs thus might not be ancestral miRNAs that were lost in other species. Rather, they represent novel miRNAs that arose specifically during the evolution of this liverwort lineage and thereby probably contributed to the wide diversity observed in this taxon.

Convergent evolution of miRNA regulation

In Arabidopsis, Ath-miR168 regulates At*AGO1*, whereas Mpo-miR11707.1 and Mpo-miR11707.2, which are generated from a single precursor, regulate Mp*AGO1*. Thus, miRNA-mediated feedback regulation of AGO1 has evolved independently in the two lineages. Interestingly, the first nucleotide of Mpo-miR11707.1 is a 'G' and this miRNA can target the Mp*AGO1* transcript in *M. polymorpha* and *N. benthamiana*. These findings suggest that certain AGO proteins might be able to load Mpo-miR11707.1. One report shows that small RNAs with G in the first position associate with AtAGO1 and AtAGO4 (Mi et al. 2008), suggesting that MpAGO1/4 might be able to load Mpo-miR11707.1 for Mp*AGO1* transcript regulation.

Lineage-specific functions

Over 100 MADS-box TFs with a conserved MADS domain (39 Type I and 69 Type II genes) that mediate DNA binding exist in Arabidopsis. Type II MADS-box genes, which are characterized by a more complex modular structure, diverged further in land plants into the MIKC^c and MIKC* lineages (Parenicová et al. 2003, Tanabe et al. 2005). MIKC^c MADS-box genes are crucial for the control of many developmental processes in flowering plants, and several of these genes have been intensively

Table 5 Comparison of miRNAs conserved across other major land plant lineages

miRNA	*Marchantia polymorpha*	*Pellia endiviifolia*	*Physcomitrella patens*	*Selaginella moellendorffii*	*Picea abies*	*Pinus taeda*	*Arabidopsis thaliana*	*Oryza sativa*
miR156/157		+	3	4		2	12	12
miR319/159	1	+	5	2 + 2		1 + 3	6	2 + 6
miR160	1	+	9	2	2		3	6
miR166/165	1	+	13	3	2	3	9	13
miR168			–	–			2	2
miR171/170	1	+	2	4		1	4	9
miR390	1	+	3	–		1	2	1
miR395		+	1	–	1		6	25
miR408	2	+	2	1		1	1	1
miR529	3		7	–			-	2
miR536			6	1			-	-

analyzed as key homeotic regulators of flower development (Smaczniak et al. 2012). Less is known regarding the functions of Type I and MIKC* genes, probably due to subtle and/or redundant functions in gametophyte, embryo and seed development in flowering plants.

Five Type I, six MIKC^c and 12 MIKC* MADS-box genes exist in *P. patens*; however, analyses of their functions have been hindered by genetic redundancies (Riese et al. 2005, Singer et al. 2007, Rensing et al. 2008). The MADS-box gene *PPM1* and two other MICK^c genes are targeted by the miRNA Ppt-MIR538a-c (Arazi 2012, Coruh et al. 2015). In *M. polymorpha*, two different miRNAs, Mpo-miR11687.1 and Mpo-miR11681.1, were identified that target Mp*MADS1*, and Mp*MADS2*, respectively. The functionality of Mpo-miR11687.1 in down-regulating Mp*MADS1* expression was demonstrated by conducting a combination of RNA and protein expression reporter assays in transiently transformed *N. benthamiana* leaves and by conducting overexpression studies of wild-type and miRNA-resistant Mp*MADS1* genes in *M. polymorpha*. Given that different, non-conserved miRNAs targeting MADS-box genes exist in *P. patens* and that no miRNAs targeting MADS-box genes in *P. endiviifolia* could be identified (Alaba et al. 2015, Coruh et al. 2015), miRNA control of MADS-box gene expression probably evolved independently within the *Marchantia* lineage. It will be interesting to unravel in the future the function of this regulatory mechanism and its impact on the establishment of the wide diversity observed in the *Marchantia* lineage.

PPR proteins in *M. polymorpha*

PPR proteins, which contain 2–30 repeats of an RNA-nucleotide binding motif, are involved in different steps of RNA metabolism, mainly in organelles, in various organisms (Barkan and Small 2014). A comparison of PPR proteins between *Marchantia* lineage and flowering plants yielded particularly interesting results; the liverwort has apparently secondarily lost the ability to conduct RNA editing, which requires approximately 200 PPR proteins of a specific subtype. The MpPPR_66 protein is of the type generally involved in mRNA processing, intron splicing and/or translation control, and its precise function remains unclear. It contains an SMR domain at the C-terminus for four PPR repeats. The gene that is most similar to Mp*PPR_66* in Arabidopsis is AT2G17033, with 29% identical amino acids. The conservation of the position of an intron among MpPPR_66, AT2G17033 and its homologs in other terrestrial plants suggests functional conservation during plant evolution. However, the functions of MpPPR_66-related proteins and their potential orthologs have not been well analyzed in flowering plants.

We demonstrate that the Mp*PPR_66* transcript has a long stem–loop that can generate Mpo-miR11692.1 to regulate its own transcription *in cis*, suggesting that a feedback loop may control its expression in vivo. An analogous structural RNA loop functions as part of a feedback loop in the Ath-miR168/At*AGO1* and Ath-miR162/At*DCL1* RNA silencing pathways (Ronemus et al. 2006, Vaucheret et al. 2006); thus MpPPR_66 might also be involved in a similar miRNA fine-tuning mechanism to regulate RNA metabolism. MpPPR_66 is predicted to localize to the chloroplast by two target prediction programs: TargetP (Emanuelsson et al. 2000) and Predotar (Small et al. 2004). The self-regulation of Mp*PPR_66* mRNA observed in this study suggests that miRNA indirectly regulates organellar RNA. Alternatively, this protein might be directly involved in RNA regulation and RNA silencing steps in the cytosol or the nucleus. The subcellular localization of the MpPPR_66 protein and its possible direct interaction with the miRNA encoded in the gene itself have to be analyzed further.

Conclusion

In this study, we demonstrated that integrating the degradome profile enhances the accuracy of the miRNA/target prediction in *M. polymorpha*. Approximately 91.5% of miRNAs of *M. polymorpha* are novel, and only 8.5% are conserved throughout embryophytes. Target genes of conserved miRNAs are sometimes orthologs in embryophytes; however, in some cases, the targets represent either paralogs or members of different gene families, suggesting complex miRNA evolution. Various *M. polymorpha* miRNA-targeted genes include those involved in gene silencing, stresses and defense responses, and lineage-specific functions were discovered and highlighted. Such discovery will help increase our knowledge of the evolution of conserved miRNAs and a broad range of lineage-specific miRNAs and their impacts on diverse plant processes.

Materials and Methods

Plant material

Male (Tak1) and female (Tak2) *M. polymorpha* plants were asexually propagated in vitro in half-strength Gamborg's B5 medium supplemented with 1% agar and maintained in a growth chamber under a 16 h light/8 h dark cycle at 25°C.

Total RNA extraction and RNA-Seq

Total RNA was extracted from 4-week-old *M. polymorpha* thalli using TRIzol reagent (Invitrogen) according to the manufacturer's protocol. Deep sequencing in this study was performed using an Illumina HiSeq 2000 by Genomics BioSci & Tech Co. In brief, poly(A) RNAs were isolated from 10 μg of total RNAs using oligo(dT) beads and fragmented by adding fragment buffer for cDNA library construction. The short RNA fragments (~200 nt) were converted to first-strand cDNA using a random hexamer and reverse transcriptase. The cDNAs were further purified using a QiaQuick PCR extraction kit (Qiagen) and were resolved in EB buffer for end repair and poly(A) tail addition. Sequencing adaptors were then ligated to the cDNAs and used as templates for PCR amplification to generate a cDNA library. The cDNA library was used for 2G nt throughput transcriptome sequence paired-end sequencing (2 × 250 nt).

To construct a cDNA library for small RNA sequencing, small RNAs (18–30 nt) were isolated from 10 μg of total RNAs using size fractionation. The size-selected small RNAs were ligated with 5′ and 3′ adaptors and then amplified by RT–PCR. The cDNA library was used for 10M nt throughput small RNA fragment sequencing (30 nt).

To construct a degradome library, poly(A) RNAs were isolated from 100 μg of total RNAs and ligated with a 5′ RNA adaptor and then converted to cDNA by RT–PCR. The PCR products were digested with *MmeI*, and then the digested 5′ portions of DNA fragments were ligated with a 3′ adaptor and further amplified by PCR. The cDNA library was used for 10M nt throughput degradome sequencing (50 nt).

Gene and miRNA target identification in *M. polymorpha*

For transcriptome database construction, trimmed reads were de novo assembled using CLC Genomics Workbench 5.1 with the default settings. Contig sequences were further analyzed to identify ORF annotations via comparison with the Arabidopsis (TAIR 10) and EMBL CDS databases using the ContigViews-transcriptome system. All the information regarding *M. polymorpha* transcriptome database construction can be accessed in the ContigViews-transcriptome system.

Whole-transcriptome contig sequences of *M. polymorpha* were used as queries for secondary structure prediction using the RNAfold program from ViennaRNA web services (rna.tbi.univie.ac.at), and the results were entered into the ContigViews-miRNA system for subsequent miRNA prediction. The miRNA prediction program from the ContigViews-miRNA system was used to analyze the small RNA and RNA folding patterns to predict miRNA precursors. The prediction pipeline includes several steps: (i) small RNA mapping: perfect identity of small RNAs to the stem region of predicted stem–loop structures was required; (ii) small RNA pairing: two small RNA pairing allows a maximum of six mismatches; (iii) 3′-end overhang on the paired small RNA structure: we allow 0–3 nt overhanging at the 3′ end of double stranded small RNA; and (iv) G:U pairing is allowed in two positions of the small RNA duplex.

Candidate miRNAs and genes were used as queries to identify potential miRNA targets using psRNAtarget [maximum expectation, 5.0; length for complementarity scoring, 20; number of top target genes for each small RNA, 200; target accessibility, 250; flanking length, 17 bp upstream and 13 bp downstream; range of central mismatch, 9–10 nt] (Dai and Zhao 2011). The prediction results were further analyzed using the miRNA target finding program of the ContigViews-miRNA system with the degradome profile. Target sites with significant degradome reads (i.e., specific accumulation of >20 unique reads at the 10th and 11th positions of the predicted site) were considered as potential target sites. Finally, all confirmed miRNAs and targets were incorporated into the ContigViews-miRNA system so that the transcriptome profile could be accessed together with the miRNA–target information.

Statistical analysis

MiRNA and degradome profiles were analyzed using CLC Genomics Workbench 5.1 (CLC Bio) and the ContigViews analysis platform. Read normalization for miRNA and degradome assays was performed using the ratio of total reads of *M. polymorpha*. The reads were mapped to the targeted degradome sequences, and the read count for each base was summarized using 't-plot', which was generated using R language. The significance of the read counts of the target site for the targeted degradome sequence was determined using the Binomial test.

Small RNA detection and β-elimination

For small RNA Northern blotting analysis, total RNA (10 μg) was separated on a 15% polyacrylamide/1 × TBE/8 M urea gel and transferred to a Hybond-N+ membrane. The miRNA antisense DNA probes (**Supplementary Table S4**) were end-labeled with [γ-P^{32}]ATP using T4 polynucleotide kinase (New England Biolabs). Free radioisotopes were filtered out using a Mini Quick Spin Oligo Column (Roche). The membrane was hybridized with ULTRAhyb®-Oligo hybridization buffer (Ambion) at 42°C for 16 h, and the signal was detected using X-film (GE Healthcare) at −80°C for 16 h.

For β-elimination, periodate treatment was performed following the method of Akbergenov et al. (2006). Briefly, total RNA was treated with 0.05 M borax/boric acid/NaOH (pH 9.5) at 45°C for 90 min. Then, the RNA was precipitated and subjected to small RNA Northern blotting analysis.

Gene cloning for the reporter assay

For the reporter assay, miRNA precursors and 120 nt target fragments of DNA containing the miRNA target sites were amplified from *M. polymorpha* cDNA by RT–PCR with specific primers (**Supplementary Table S5, S6**) and cloned into the pENTR/D-TOPO vector (Invitrogen). These miRNA genes in pENTR vectors were then transferred into the pBCo-DC-myc binary vector using LR Clonase (Gateway system, Invitrogen). In addition, various 120 nt target fragments in the pENTR vector were transferred into the pBCo-DC-YFP binary vector via LR reaction. These binary plasmids were transformed into *Agrobacterium tumefaciens* strain ABI for transient expression in *N. benthamiana* by agroinfiltration.

Transient expression by agroinfiltration

Agrobacterium tumefaciens strain ABI containing a binary vector was incubated in LB medium with 10 mM MES (pH 5.6), 40 μM acetosyringone, 100 μg ml^{-1} spectinomycin and 50 μg ml^{-1} kanamycin at 28°C for 16 h. The cultures were then centrifuged, and the agrobacteria were resuspended with the appropriate buffer (10 mM $MgCl_2$ and 150 μM acetosyringone) to adjust the absorbance to OD_{600} = 0.5. The agrobacteria were then incubated at room temperature for 3 h (Lin et al. 2013). Agrobacteria carrying Mp*MIR* genes or target fragment-*YFP* recombinant genes were mixed (miRNA : target = 2 : 1) and used for the co-infiltration of *N. benthamiana* plants. Four days post-infiltration, the infiltrated *N. benthamiana* leaves were collected and analyzed by real-time RT–PCR and Northern blot.

To assess the reporter assay results, YFP fluorescence in the infiltrated leaves was monitored using a Leica TCS SP5 II confocal laser-scanning microscope (Joint Center for Instruments and Researches, College of Bioresources and Agriculture, National Taiwan University) equipped with a multiline argon laser with a filter set for YFP fluorescence [excitation filter Acousto-optic Tunable filter 488, emission bandwidth 496–574 nm, PMT2 offset (−1.0)/gain (895.0)]. All images were organized using Adobe Photoshop CS3 software (Adobe Systems Inc.).

Mp*MADS1* overexpression in *M. polymorpha* and real-time RT–PCR

Mp*MADS1* and Mpo-miR11687.1-resistant Mp$MADS1^{mut}$ cDNAs were expressed in *M. polymorpha* (BoGa ecotype, Osnabrück) under the control of the *EF1α* promoter (Althoff et al. 2014). Seven synonymous changes were introduced in the Mpo-miR11687.1 target site by overlap-PCR using two primer pairs (5′-CACCATGGGGAGGGTCAAGCT-3′/5′-CGCTTTGTTTAAGTATTCTAAGTTTTCGAATTTTC-3′ and 5′-GAAAATTCGAAAACTTAGAATACTTAAACAAAGCG-3′/5′-TCACGGATTGTAGTAATTGGGTG-3′) to generate Mp$MADS1^{mut}$. Both cDNAs were cloned in the pGWB2 vector and transformed into *M. polymorpha*. Wild-type expression was assessed in two independent lines carrying the empty pGWB2 vector, and three independent transgenic *M. polymorpha* plants were analyzed for each construct. The primers 5′-AACCGGCAGGTCACATACTC-3′ and 5′-CGAGAACATGATAACCGCAAT-3′ were used for cDNA amplification of Mp*MADS1*/Mp$MADS1^{mut}$, and the primers 5′-CTTCGTGCCAATTTCTGGAT-3′ and 5′-GCTCACTGATGCTGTCCAAA-3′ were used for amplification of *EF1α*, which served as a reference gene. The mean normalized expression (MNE) of three technical replicates was averaged, and the SEs were calculated. The MNE of the wild-type plants was set to 1, and relative expression values were determined for the overexpression lines.

Supplementary data

Supplementary data are available at PCP online.

Funding

This study was supported by the Ministry of Science and Technology (grant Nos. MOST 104-2321-B-002-064 and MOST 102-2313-B-002-068-MY3].

Disclosures

The authors have no conflicts of interest to declare.

References

Addo-Quaye, C., Eshoo, T.W., Bartel, D.P. and Axtell, M.J. (2008) Endogenous siRNA and miRNA targets identified by sequencing of the Arabidopsis degradome. *Curr. Biol.* 18: 758–762.

Akbergenov, R., Si-Ammour, A., Blevins, T., Amin, I., Kutter, C., Vanderschuren, H., et al. (2006) Molecular characterization of geminivirus-derived small RNAs in different plant species. *Nucleic Acids Res.* 34: 462–471.

Alaba, S., Piszczalka, P., Pietrykowska, H., Pacak, A.M., Sierocka, I., Nuc, P.W., et al. (2015) The liverwort *Pellia endiviifolia* shares microtranscriptomic traits that are common to green algae and land plants. *New Phytol.* 206: 352–367.

Allen, E., Xie, Z., Gustafson, A.M. and Carrington, J.C. (2005) microRNA-directed phasing during trans-acting siRNA biogenesis in plants. *Cell* 121: 207–221.

Althoff, F., Kopischke, S., Zobell, O., Ide, K., Ishizaki, K., Kohchi, T., et al. (2014) Comparison of the MpEF1α and CaMV35 promoters for application in *Marchantia polymorpha* overexpression studies. *Transgenic Res.* 23: 235–244.

Anderson, H.M. (1976) A review of the Bryophyta from the Upper Triassic Molteno Formation, Karoo Basin, South Africa. *Palaeont. Afr.* 19: 21–30.

Arazi, T. (2012) MicroRNAs in the moss *Physcomitrella patens*. *Plant Mol. Biol.* 80: 55–65.

Aukerman, M.J. and Sakai, H. (2003) Regulation of flowering time and floral organ identity by a MicroRNA and its *APETALA2-like* target genes. *Plant Cell* 15: 2730–2741.

Axtell, M.J., Snyder, J.A. and Bartel, D.P. (2007) Common functions for diverse small RNAs of land plants. *Plant Cell* 19: 1750–1769.

Bardou, F., Ariel, F., Simpson, C.G., Romero-Barrios, N., Laporte, P., Balzergue, S., et al. (2014) Long noncoding RNA modulates alternative splicing regulators in Arabidopsis. *Dev. Cell* 30: 166–176.

Barkan, A. and Small, I. (2014) Pentatricopeptide repeat proteins in plants. *Annu. Rev. Plant Biol.* 65: 415–442.

Bartel, D.P. (2004) MicroRNAs: genomics, biogenesis, mechanism, and function. *Cell* 116: 281–297.

Baumberger, N. and Baulcombe, D.C. (2005) Arabidopsis ARGONAUTE1 is an RNA Slicer that selectively recruits microRNAs and short interfering RNAs. *Proc. Natl. Acad. Sci. USA* 102: 11928–11933.

Bowman, J.L. (2013) Walkabout on the long branches of plant evolution. *Curr. Opin. Plant Biol.* 16: 70–77.

Bracken, C.P., Szubert, J.M., Mercer, T.R., Dinger, M.E., Thomson, D.W., Mattick, J.S., et al. (2011) Global analysis of the mammalian RNA degradome reveals widespread miRNA-dependent and miRNA-independent endonucleolytic cleavage. *Nucleic Acids Res.* 39: 5658–5668.

Campalans, A., Kondorosi, A. and Crespi, M. (2004) Enod40, a short open reading frame-containing mRNA, induces cytoplasmic localization of a nuclear RNA binding protein in Medicago truncatula. *Plant Cell* 16: 1047–1059.

Cao, X., Wu, Z., Jiang, F., Zhou, R. and Yang, Z. (2014) Identification of chilling stress-responsive tomato microRNAs and their target genes by high-throughput sequencing and degradome analysis. *BMC Genomics* 15: 1130.

Chen, X. (2009) Small RNAs and their roles in plant development. *Annu. Rev. Cell Dev. Biol.* 25: 21–44.

Chen, X. (2012) Small RNAs in development—insights from plants. *Curr. Opin. Genet. Dev.* 22: 361–367.

Coruh, C., Cho, S.H., Shahid, S., Liu, Q., Wierzbicki, A. and Axtell, M.J. (2015) Comprehensive annotation of *Physcomitrella patens* small RNA loci reveals that the heterochromatic short interfering RNA pathway is largely conserved in land plants. *Plant Cell* 27: 2148–2162.

Cuperus, J.T., Fahlgren, N. and Carrington, J.C. (2011) Evolution and functional diversification of MIRNA genes. *Plant Cell* 23: 431–442.

Dai, X. and Zhao, P.X. (2011) psRNATarget: a plant small RNA target analysis server. *Nucleic Acids Res.* 39: W155–W159.

Daram, P., Brunner, S., Rausch, C., Steiner, C., Amrhein, N. and Bucher, M. (1999) Pht2;1 encodes a low-affinity phosphate transporter from Arabidopsis. *Plant Cell* 11: 2153–2166.

Ding, J., Lu, Q., Ouyang, Y., Mao, H., Zhang, P., Yao, J., et al. (2012) A long noncoding RNA regulates photoperiod-sensitive male sterility, an essential component of hybrid rice. *Proc. Natl. Acad. Sci. USA* 109: 2654–2659.

Emanuelsson, O., Nielsen, H., Brunak, S. and von Heijne, G. (2000) Predicting subcellular localization of proteins based on their N-terminal amino acid sequence. *J. Mol. Biol.* 300: 1005–1016.

Emery, J.F., Floyd, S.K., Alvarez, J., Eshed, Y., Hawker, N.P., Izhaki, A., et al. (2003) Radial patterning of Arabidopsis shoots by *class III HD-ZIP* and *KANADI* genes. *Curr. Biol.* 13: 1768–1774.

Eulgem, T., Tsuchiya, T., Wang, X.J., Beasley, B., Cuzick, A., Tör, M., et al. (2007) EDM2 is required for RPP7-dependent disease resistance in Arabidopsis and affects RPP7 transcript levels. *Plant J.* 49: 829–839.

Fahlgren, N., Howell, M.D., Kasschau, K.D., Chapman, E.J., Sullivan, C.M., Cumbie, J.S., et al. (2007) High-throughput sequencing of Arabidopsis microRNAs: evidence for frequent birth and death of MIRNA genes. *PLoS One* 2: e219.

Fahlgren, N., Jogdeo, S., Kasschau, K.D., Sullivan, C.M., Chapman, E.J., Laubinger, S., et al. (2010) MicroRNA gene evolution in *Arabidopsis lyrata* and *Arabidopsis thaliana*. *Plant Cell* 22: 1074–1089.

Fahlgren, N., Montgomery, T.A., Howell, M.D., Allen, E., Dvorak, S.K., Alexander, A.L., et al. (2006) Regulation of *AUXIN RESPONSE FACTOR3* by *TAS3* ta-siRNA affects developmental timing and patterning in Arabidopsis. *Curr. Biol.* 16: 939–944.

Fattash, I., Voss, B., Reski, R., Hess, W.R. and Frank, W. (2007) Evidence for the rapid expansion of microRNA-mediated regulation in early land plant evolution. *BMC Plant Biol.* 7: 13.

Fei, Q., Xia, R. and Meyers, B.C. (2013) Phased, secondary, small interfering RNAs in posttranscriptional regulatory networks. *Plant Cell* 25: 2400–2415.

Feldberg, K., Schneider, H., Stadler, T., Schäfer-Verwimp, A., Schmidt, A.R. and Heinrichs, J. (2014) Epiphytic leafy liverworts diversified in angiosperm-dominated forests. *Sci. Rep.* 4: 5974.

Flores-Sandoval, E., Dierschke, T., Fisher, T.J. and Bowman, J.L. (2016) Efficient and inducible use of artificial microRNAs in *Marchantia polymorpha*. *Plant Cell Physiol.* 57: 281–290.

Floyd, S.K. and Bowman, J.L. (2004) Gene regulation: ancient microRNA target sequences in plants. *Nature* 428: 485–486.

Floyd, S.K., Zalewski, C.S. and Bowman, J.L. (2006) Evolution of class III homeodomain-leucine zipper genes in streptophytes. *Genetics* 173: 373–388.

Gensel, P.G. (2008) The earliest land plants. *Annu. Rev. Ecol. Evol.* 39: 459–477.

German, M.A., Luo, S., Schroth, G., Meyers, B.C. and Green, P.J. (2009) Construction of Parallel Analysis of RNA Ends (PARE) libraries for the study of cleaved miRNA targets and the RNA degradome. *Nat. Protoc.* 4: 356–362.

German, M.A., Pillay, M., Jeong, D.H., Hetawal, A., Luo, S., Janardhanan, P., et al. (2008) Global identification of microRNA–target RNA pairs by parallel analysis of RNA ends. *Nat. Biotechnol.* 26: 941–946.

Gregory, B.D., O'Malley, R.C., Lister, R., Urich, M.A., Tonti-Filippini, J., Chen, H., et al. (2008) A link between RNA metabolism and silencing affecting Arabidopsis development. *Dev. Cell* 14: 854–866.

Heo, J.B. and Sung, S. (2011) Vernalization-mediated epigenetic silencing by a long intronic noncoding RNA. *Science* 331: 76–79.

Hunter, C., Willmann, M.R., Wu, G., Yoshikawa, M., de la Luz Gutiérrez-Nava, M. and Poethig, S.R. (2006) Trans-acting siRNA-mediated repression of *ETTIN* and *ARF4* regulates heteroblasty in Arabidopsis. *Development* 133: 2973–2981.

Iuchi, S., Koyama, H., Iuchi, A., Kobayashi, Y., Kitabayashi, S., Kobayashi, Y., et al. (2007) Zinc finger protein STOP1 is critical for proton tolerance in Arabidopsis and coregulates a key gene in aluminum tolerance. *Proc. Natl. Acad. Sci. USA* 104: 9900–9905.

Jabnoune, M., Secco, D., Lecampion, C., Robaglia, C., Shu, Q. and Poirier, Y. (2013) A rice cis-natural antisense RNA acts as a translational enhancer for its cognate mRNA and contributes to phosphate homeostasis and plant fitness. *Plant Cell* 25: 4166–4182.

Jeong, D.H., Schmidt, S.A., Rymarquis, L.A., Park, S., Ganssmann, M., German, M.A., et al. (2013) Parallel analysis of RNA ends enhances global investigation of microRNAs and target RNAs of Brachypodium distachyon. *Genome Biol.* 14: R145.

Kato, H., Ishizaki, K., Kouno, M., Shirakawa, M., Bowman, J.L., Nishihama, R., et al. (2015) Auxin-mediated transcriptional system with a minimal set of components is critical for morphogenesis through the life cycle in *Marchantia polymorpha*. *PLoS Genet.* 11: e1005084.

Kenrick, P. and Crane, P.R. (1997) The origin and early evolution of plants on land. *Nature* 389: 33–39.

Kim, V.N. and Nam, J.W. (2006) Genomics of microRNA. *Trends Genet.* 22: 165–173.

Kim, Y.J., Zheng, B., Yu, Y., Won, S.Y., Mo, B. and Chen, X. (2011) The role of Mediator in small and long noncoding RNA production in *Arabidopsis thaliana*. *EMBO J.* 30: 814–822.

Komatsu, A., Terai, M., Ishizaki, K., Suetsugu, N., Tsuboi, H., Nishihama, R., et al. (2014) Phototropin encoded by a single-copy gene mediates chloroplast photorelocation movements in the liverwort *Marchantia polymorpha*. *Plant Physiol.* 166: 411–427.

Kozomara, A. and Griffiths-Jones, S. (2011) miRBase: integrating microRNA annotation and deep-sequencing data. *Nucleic Acids Res.* 39: D152–D157.

Krasnikova, M.S., Goryunov, D.V., Troitsky, A.V., Solovyev, A.G., Ozerova, L.V. and Morozov, S.Y. (2013) Peculiar evolutionary history of miR390-guided TAS3-like genes in land plants. *ScientificWorldJournal* 2013: 924153.

Lai, E.C., Wiel, C. and Rubin, G.M. (2004) Complementary miRNA pairs suggest a regulatory role for miRNA:miRNA duplexes. *RNA* 10: 171–175.

Lampl, N., Alkan, N., Davydov, O. and Fluhr, R. (2013) Set-point control of RD21 protease activity by AtSerpin1 controls cell death in Arabidopsis. *Plant J.* 74: 498–510.

Law, J.A. and Jacobsen, S.E. (2010) Establishing, maintaining and modifying DNA methylation patterns in plants and animals. *Nat. Rev. Genet.* 11: 204–220.

Lee, R.C., Feinbaum, R.L. and Ambros, V. (1993) The *C. elegans* heterochronic gene *lin-4* encodes small RNAs with antisense complementarity to *lin-14*. *Cell* 75: 843–854.

Lei, M., La, H., Lu, K., Wang, P., Miki, D., Ren, Z., et al. (2014) Arabidopsis EDM2 promotes *IBM1* distal polyadenylation and regulates genome DNA methylation patterns. *Proc. Natl. Acad. Sci. USA* 111: 527–532.

Ligrone, R., Duckett, J.G. and Renzaglia, K.S. (2012) Major transitions in the evolution of early land plants: a bryological perspective. *Ann. Bot.* 109: 851–871.

Lin, Y.Y., Fang, M.M., Lin, P.C., Chiu, M.T., Liu, L.Y., Lin, C.P., et al. (2013) Improving initial infectivity of the *Turnip mosaic virus* (TuMV) infectious clone by an mini binary vector via agro-infiltration. *Bot. Stud.* 54: 22.

Liu, L.Y., Tseng, H.I., Lin, C.P., Lin, Y.Y., Huang, Y.H., Huang, C.K., et al. (2014) High-throughput transcriptome analysis of the leafy flower transition of *Catharanthus roseus* induced by peanut witches'-broom phytoplasma infection. *Plant Cell Physiol.* 55: 942–957.

Liu, Y., Geyer, R., van Zanten, M., Carles, A., Li, Y., Hörold, A., et al. (2011) Identification of the Arabidopsis *REDUCED DORMANCY 2* gene uncovers a role for the polymerase associated factor 1 complex in seed dormancy. *PLoS One* 6: e22241.

Lu, C., Jeong, D.H., Kulkarni, K., Pillay, M., Nobuta, K., German, R., et al. (2008) Genome-wide analysis for discovery of rice microRNAs reveals natural antisense microRNAs (nat-miRNAs). *Proc. Natl. Acad. Sci. USA* 105: 4951–4956.

Ma, Z., Coruh, C. and Axtell, M.J. (2010) *Arabidopsis lyrata* small RNAs: transient MIRNA and small interfering RNA loci within the Arabidopsis genus. *Plant Cell* 22: 1090–1103.

Mallory, A. and Vaucheret, H. (2010) Form, function, and regulation of ARGONAUTE proteins. *Plant Cell* 22: 3879–3889.

Mallory, A.C., Dugas, D.V., Bartel, D.P. and Bartel, B. (2004) MicroRNA regulation of NAC-domain targets is required for proper formation and separation of adjacent embryonic, vegetative, and floral organs. *Curr. Biol.* 14: 1035–1046.

Marin, E., Jouannet, V., Herz, A., Lokerse, A.S., Weijers, D., Vaucheret, H., et al. (2010) miR390, Arabidopsis *TAS3* tasiRNAs, and their *AUXIN RESPONSE FACTOR* targets define an autoregulatory network quantitatively regulating lateral root growth. *Plant Cell* 22: 1104–1117.

Matzke, M.A., Kanno, T. and Matzke, A.J. (2015) RNA-directed DNA methylation: the evolution of a complex epigenetic pathway in flowering plants. *Annu. Rev. Plant Biol.* 66: 243–267.

Matzke, M.A. and Mosher, R.A. (2014) RNA-directed DNA methylation: an epigenetic pathway of increasing complexity. *Nat. Rev. Genet.* 2014: 394–408.

McConnell, J.R., Emery, J., Eshed, Y., Bao, N., Bowman, J. and Barton, M.K. (2001) Role of PHABULOSA and PHAVOLUTA in determining radial patterning in shoots. *Nature* 411: 709–713.

Mi, S., Cai, T., Hu, Y., Chen, Y., Hodges, E., Ni, F., et al. (2008) Sorting of small RNAs into Arabidopsis argonaute complexes is directed by the 5′ terminal nucleotide. *Cell* 133: 116–127.

Mishler, B.D. and Churchill, S.P. (1984) A cladistic approach to the phylogeny of the 'Bryophytes'. *Brittonia* 36: 406–424.

Nagai, J., Yamato, K.T., Sakaida, M., Yoda, H., Fukuzawa, H. and Ohyama, K. (1999) Expressed sequence tags from immature female sexual organ of a liverwort, *Marchantia polymorpha*. *DNA Res.* 26: 1–11.

Nishiyama, R., Yamato, K.T., Miura, K., Sakaida, M., Okada, S., Kono, K., et al. (2000) Comparison of expressed sequence tags from male and female sexual organs of *Marchantia polymorpha*. *DNA Res.* 7: 165–174.

Parenicová, L., de Folter, S., Kieffer, M., Horner, D.S., Favalli, C., Busscher, J., et al. (2003) Molecular and phylogenetic analyses of the complete MADS-box transcription factor family in Arabidopsis: new openings to the MADS world. *Plant Cell* 15: 1538–1551.

Pattanayak, G.K., Venkataramani, S., Hortensteiner, S., Kunz, L., Christ, B., Moulin, M., et al. (2012) Accelerated cell death 2 suppresses mitochondrial oxidative bursts and modulates cell death in Arabidopsis. *Plant J.* 69: 589–600.

Peragine, A., Yoshikawa, M., Wu, G., Albrecht, H.L. and Poethig, R.S. (2004) SGS3 and SGS2/SDE1/RDR6 are required for juvenile development and the production of trans-acting siRNAs in Arabidopsis. *Genes Dev.* 18: 2368–2379.

Prigge, M.J. and Clark, S.E. (2006) Evolution of the *class III HD-Zip* gene family in land plants. *Evol. Dev.* 8: 350–361.

Qiu, Y.L., Li, L., Wang, B., Chen, Z., Knoop, V., Groth-Malonek, M., et al. (2006) The deepest divergences in land plants inferred from phylogenomic evidence. *Proc. Natl. Acad. Sci. USA* 103: 15511–15516.

Rajagopalan, R., Vaucheret, H., Trejo, J. and Bartel, D.P. (2006) A diverse and evolutionarily fluid set of microRNAs in Arabidopsis thaliana. *Genes Dev.* 20: 3407–3425.

Reinhart, B.J., Weinstein, E.G., Rhoades, M.W., Bartel, B. and Bartel, D.P. (2002) MicroRNAs in plants. *Genes Dev.* 16: 1616–1626.

Rensing, S.A., Lang, D., Zimmer, A.D., Terry, A., Salamov, A., Shapiro, H., et al. (2008) The Physcomitrella genome reveals evolutionary insights into the conquest of land by plants. *Science* 319: 64–69.

Riese, M., Faigl, W., Quodt, V., Verelst, W., Matthes, A., Saedler, H., et al. (2005) Isolation and characterization of new MIKC*-Type MADS-box genes from the moss *Physcomitrella patens*. *Plant Biol.* 7: 307–314.

Rinn, J.L. and Chang, H.Y. (2012) Genome regulation by long noncoding RNAs. *Annu. Rev. Biochem.* 81: 145–166.

Rogers, K. and Chen, X. (2013) Biogenesis, turnover, and mode of action of plant microRNAs. *Plant Cell* 25: 2383–2399.

Ronemus, M., Vaughn, M.W. and Martienssen, R.A. (2006) MicroRNA-targeted and small interfering RNA-mediated mRNA degradation is regulated by argonaute, dicer, and RNA-dependent RNA polymerase in Arabidopsis. *Plant Cell* 18: 1559–1574.

Sanei, M. and Chen, X. (2015) Mechanisms of microRNA turnover. *Curr. Opin. Plant Biol.* 27: 199–206.

Sharma, N., Jung, C.H., Bhalla, P.L. and Singh, M.B. (2014) RNA sequencing analysis of the gametophyte transcriptome from the liverwort, *Marchantia polymorpha*. *PLoS One* 9: e97497.

Singer, S.D., Krogan, N.T. and Ashton, N.W. (2007) Clues about the ancestral roles of plant *MADS-box* genes from a functional analysis of moss homologues. *Plant Cell Rep.* 26: 1155–1169.

Smaczniak, C., Immink, R.G., Angenent, G.C. and Kaufmann, K. (2012) Developmental and evolutionary diversity of plant MADS-domain factors: insights from recent studies. *Development* 139: 3081–3098.

Small, I., Peeters, N., Legeai, F. and Lurin, C. (2004) Predotar: a tool for rapidly screening proteomes for N-terminal targeting sequences. *Proteomics* 4: 1581–1590.

Tanabe, Y., Hasebe, M., Sekimoto, H., Nishiyama, T., Kitani, M., Henschel, K., et al. (2005) Characterization of MADS-box genes in charophycean green algae and its implication for the evolution of MADS-box genes. *Proc. Natl. Acad. Sci. USA* 102: 2436–2441.

Vaucheret, H., Mallory, A.C. and Bartel, D.P. (2006) AGO1 homeostasis entails coexpression of MIR168 and AGO1 and preferential stabilization of miR168 by AGO1. *Mol. Cell* 22: 129–136.

Vazquez, F., Vaucheret, H., Rajagopalan, R., Lepers, C., Gasciolli, V., Mallory, A.C., et al. (2004) Endogenous trans-acting siRNAs regulate the accumulation of Arabidopsis mRNAs. *Mol. Cell* 16: 69–79.

Walton, J. (1925) Carboniferous bryophyta. I. Hepaticae. *Ann. Bot.* 39: 563–572.

Wang, Y., Fan, X., Lin, F., He, G., Terzaghi, W., Zhu, D., et al. (2014) Arabidopsis noncoding RNA mediates control of photomorphogenesis by red light. *Proc. Natl. Acad. Sci. USA* 111: 10359–10364.

Werner, M.S. and Ruthenburg, A.J. (2015) Nuclear fractionation reveals thousands of chromatin-tethered noncoding RNAs adjacent to active genes. *Cell Rep.* 12: 1089–1098.

Wightman, B., Ha, I. and Ruvkun, G. (1993) Posttranscriptional regulation of the heterochronic gene lin-14 by lin-4 mediates temporal pattern formation in *C. elegans*. *Cell* 75: 855–862.

Williams, L., Carles, C.C., Osmont, K.S. and Fletcher, J.C. (2005) A database analysis method identifies an endogenous trans-acting short-interfering RNA that targets the Arabidopsis *ARF2*, *ARF3*, and *ARF4* genes. *Proc. Natl. Acad. Sci. USA* 102: 9703–9708.

Yang, C.Y., Huang, Y.H., Lin, C.P., Lin, Y.Y., Hsu, H.C., Wang, C.N., et al. (2015) MiR396-targeted *SHORT VEGETATIVE PHASE* is required to repress flowering and is related to the development of abnormal flower symptoms by the PHYL1 effector. *Plant Physiol.* 168: 1702–1716.

Yang, J., Liu, X., Xu, B., Zhao, N., Yang, X. and Zhang, M. (2013) Identification of miRNAs and their targets using high-throughput sequencing and degradome analysis in cytoplasmic male-sterile and its maintainer fertile lines of Brassica juncea. *BMC Genomics* 14: 9.

Yang, Z., Ebright, Y.W., Yu, B. and Chen, X. (2006) HEN1 recognizes 21–24 nt small RNA duplexes and deposits a methyl group onto the 2′ OH of the 3′ terminal nucleotide. *Nucleic Acids Res.* 34: 667–675.

Yao, F., Zhu, H., Yi, C., Qu, H. and Jiang, Y. (2015) MicroRNAs and targets in senescent litchi fruit during ambient storage and post-cold storage shelf life. *BMC Plant Biol.* 15: 181.

Yoshikawa, M. (2013) Biogenesis of trans-acting siRNAs, endogenous secondary siRNAs in plants. *Genes Genet. Syst.* 88: 77–84.

Yoshikawa, M., Peragine, A., Park, M.Y. and Poethig, R.S. (2005) A pathway for the biogenesis of trans-acting siRNAs in Arabidopsis. *Genes Dev.* 19: 2164–2175.

Yu, B., Chapman, E.J., Yang, Z., Carrington, J.C. and Chen, X. (2006) Transgenically expressed viral RNA silencing suppressors interfere with microRNA methylation in Arabidopsis. *FEBS Lett.* 580: 3117–3120.

Zhao, Z., Yu, Y., Meyer, D., Wu, C. and Shen, W.H. (2005) Prevention of early flowering by expression of *FLOWERING LOCUS C* requires methylation of histone H3 K36. *Nat. Cell Biol.* 7: 1256–1260.

Zimmer, A.D., Lang, D., Buchta, K., Rombauts, S., Nishiyama, T., Hasebe, M., et al. (2013) Reannotation and extended community resources for the genome of the non-seed plant Physcomitrella patens provide insights into the evolution of plant gene structures and functions. *BMC Genomics* 14: 498.